CREEP DAMAGE ANALYSIS AND NUMERICAL SIMULATION ON OIL WELL STEEL PIPE CASING AT ELEVATED TEMPERATURES

SARMAD KHUBAIB BIN SARAJUN HODA

FACULTY OF ENGINEERING
UNIVERSITY OF MALAYA
KUALA LUMPUR

2021

CREEP DAMAGE ANALYSIS AND NUMERICAL SIMULATION ON OIL WELL STEEL PIPE CASING AT ELEVATED TEMPERATURES

SARMAD KHUBAIB BIN SARAJUN HODA

RESEARCH REPORT SUBMITTED IN FULFILMENT OF THE REQUIREMENTS FOR THE DEGREE OF MASTER OF MECHANICAL ENGINEERING

FACULTY OF ENGINEERING
UNIVERSITY OF MALAYA
KUALA LUMPUR

2021

UNIVERSITY OF MALAYA

ORIGINAL LITERARY WORK DECLARATION

Name of Candidate: **Sarmad Khubaib Bin Sarajun Hoda**

Matric No: **17219530/1**

Name of Degree: **Master of Mechanical Engineering**

Title of ~~Project Paper~~/Research Report/~~Dissertation/Thesis~~ ("this Work"): **Creep Damage Analysis and Numerical Simulation on Oil Well Steel Pipe Casing at Elevated Temperatures**

Field of Study: **Materials**

I do solemnly and sincerely declare that:

(1) I am the sole author/writer of this Work;
(2) This Work is original;
(3) Any use of any work in which copyright exists was done by way of fair dealing and for permitted purposes and any excerpt or extract from, or reference to or reproduction of any copyright work has been disclosed expressly and sufficiently and the title of the Work and its authorship have been acknowledged in this Work;
(4) I do not have any actual knowledge nor do I ought reasonably to know that the making of this work constitutes an infringement of any copyright work;
(5) I hereby assign all and every rights in the copyright to this Work to the University of Malaya ("UM"), who henceforth shall be owner of the copyright in this Work and that any reproduction or use in any form or by any means whatsoever is prohibited without the written consent of UM having been first had and obtained;
(6) I am fully aware that if in the course of making this Work I have infringed any copyright whether intentionally or otherwise, I may be subject to legal action or any other action as may be determined by UM.

Candidate's Signature Date: 08/06/2021

Subscribed and solemnly declared before,

Witness's Signature Date:

Name:

Designation:

ABSTRACT

The purpose of this study was to investigate the Creep Damage Analysis and Numerical Simulation on Oil Well Steel Pipe casing at Elevated Temperatures using ANSYS (Computational Structural Analysis). Creep deformation is a type of plastic deformation of solid materials which occurs under high constant stress at high temperatures. Primary purpose of an Oil Well casing is to transport crude oil to the surface as well as separates the fluid or solid of inside the wellbore from the outside environment, whether in solid or in water. Casings of an oil well can experience tremendous pressure change during hydraulic fracturing processes or steam injection processes. The operating loads added with harsh conditions deep beneath the ground or in seawater exerts very high stresses on casings throughout their lifetime Analysis suggest that numerous failures of the casings have been scrutinised, however they only shed minor lights in terms on how these failures occur in terms of the life. Wellhead uplift was detected among some oil wells, and development of offshore thermal recovery technology could be restricted by the serious safety problems behind. This paper is based on the specific operating conditions of one oil well in the trial block, and the simulation calculation of casing elongation and wellhead uplift are conducted by using finite element analysis. The total casing elongation calculated is *4.2 cm*. According to the research, we concluded that the wellhead uplift is caused by upper casing elongation. 88% of the total elongation happens in the air and seawater sections. Elongation is lesser in strata and the casing string below *360 m* can be considered as anchored. The maximum total deformation was $1.4645 \times 10^{-7} m$, average elastic strain was 1.084×10^{-8} *m/m*, whereas the average volumetric change is $0.30042\ m^3$.

ABSTRAK

Tujuan kajian ini adalah untuk mengkaji Analisis Kerosakan Creep dan Simulasi Numerik pada selongsong Paip Baja Sumur Minyak pada Suhu Tertinggi menggunakan ANSYS (Analisis Struktural Komputasi). Deformation creep adalah sejenis ubah bentuk plastik bahan pepejal yang berlaku di bawah tekanan berterusan tinggi pada suhu tinggi. Tujuan utama selongsong Sumur Minyak adalah untuk mengangkut minyak mentah ke permukaan serta memisahkan bendalir atau pepejal di dalam sumur dari persekitaran luar, sama ada dalam pepejal atau di dalam air. Casing sumur minyak dapat mengalami perubahan tekanan yang luar biasa semasa proses keretakan hidraulik atau proses suntikan wap. Beban operasi ditambahkan dengan keadaan yang keras di bawah tanah atau di air laut memberikan tekanan yang sangat tinggi pada selongsong sepanjang hayatnya Analisis menunjukkan bahawa banyak kegagalan selongsong telah diteliti, namun mereka hanya memberi cahaya kecil dari segi bagaimana kegagalan ini terjadi dari segi kehidupan. Peningkatan Wellhead dikesan di antara beberapa sumur minyak, dan pengembangan teknologi pemulihan terma lepas pantai dapat dihalang oleh masalah keselamatan yang serius di belakang. Makalah ini didasarkan pada keadaan operasi khusus satu telaga minyak di blok percubaan, dan pengiraan simulasi pemanjangan selongsong dan peningkatan kepala sumur dilakukan dengan menggunakan analisis elemen. Jumlah pemanjangan selongsong yang dikira ialah *4.2 cm*. Menurut penyelidikan, kami menyimpulkan bahawa kenaikan kepala sumur disebabkan oleh pemanjangan selongsong atas. 88% daripada jumlah pemanjangan berlaku di bahagian udara dan air laut. Pemanjangan lebih kecil pada strata dan tali selongsong di bawah *360 m* dapat dianggap berlabuh. Deformasi total maksimum ialah *1.4645 x 10-7m*, tegangan elastik purata ialah *1.084 x 10-8 m/m*, sedangkan perubahan volumetrik rata-rata adalah *0.30042 m3*.

ACKNOWLEDGEMENTS

First and foremost, I would like to express my sincere gratitude to my respectful supervisor Associate Professor Madya Ir. Dr. Wong Yew Hoong for his continuous support, guidance and mentorship in completing this Research Project, as part of the fulfilment of my Master of Mechanical Engineering postgraduate studies and related researches. His patience, motivation, and immense knowledge have guided and assisted me to complete this project on time.

In general, I am very grateful and thankful to University of Malaya for continuous offering and facilitating the Master of Mechanical Engineering postgraduate program to inculcate the life-long learning practices and as well as provide working adults an opportunity to further study to update with new knowledge, while recapitulating lessons learned in undergraduate.

My sincere appreciation also extends to all my professors and lecturers for conducting and facilitating the postgraduate program professionally; and my fellow course-mates for sharing their thoughts constructively along the postgraduate learning journey. All of their advice and guidance are very useful indeed. Unfortunately, it is not possible to list all of them one by one in this limited space.

Last but not the least, my truthful appreciation goes to my family for their continuous encouragement and restlessness support throughout my postgraduate study. I am able to complete this research project and subsequently the postgraduate program as a whole, with the patience, trust and freedom given by them.

TABLE OF CONTENTS

Abstract ...iii

Abstrak ...iv

Acknowledgements ...v

Table of Contents ...vi

List of Figures ...ix

List of Tables...xii

List of Symbols and Abbreviations...xiii

List of Appendices ...xiv

CHAPTER 1: INTRODUCTION ...1

1.1 Background...1

1.2 Research Background ...6

1.3 Research Problem ...9

1.4 Research Questions...11

1.5 Research Objective ...11

1.6 Research Significance...12

1.7 Operational Definitions ...12

1.7.1 Creep Damage ...12

1.7.2 Numerical simulation ...13

1.8 Summary...13

CHAPTER 2: LITERATURE REVIEW...15

2.1 Introduction...15

2.2 Numerical Simulation of Casing Centralisation ...20

2.3 Casing integrity challenge in different well types ...23

2.3.1 HPHT & geothermal wells ... 24
2.3.2 Shale gas horizontal wells ... 25
2.3.3 Deepwater wells ... 29
2.3.4 Injection wells ... 30
2.3.5 Steam injection for heave oil recovery ... 31
2.3.6 Choosing J55 Standard oil well steel casing pipe. ... 32
2.3.6.1 Applications ... 33
2.3.6.2 Properties ... 33
2.4 Current Advances ... 34
2.5 Creep Damage Analysis and Numerical Simulation on oil well steel pipe ... 35
2.6 Overview of failure modes ... 37
2.6.1 Buckling failure or deformation ... 37
2.6.2 Shear Failure ... 39
2.6.3 Collapse or burst failure ... 40
2.6.4 Fatigue Failure ... 42
2.6.5 Wear/erosion/corrosion failure ... 44
2.6.6 Connection failure ... 46
2.6.7 Casing – cement-formation failure ... 48
2.7 Summary ... 50

CHAPTER 3: METHODOLOGY ... 53
3.1 Material characterisation ... 53
3.2 Simulation and Elongation Calculation Methods ... 54
3.3 Simulation and elongation calculation method for API 5CT J55 casing ... 55
3.4 Simulations Conditions ... 58
3.4.1 Geometry (Simulations Sample Dimensions) ... 58
3.4.2 Material Properties ... 59

3.4.3 Analysis Settings (Structural) ... 60
3.4.4 Thermal Conditions ... 60
3.5 Summary ... 61

CHAPTER 4: RESULT AND DISCUSSION ... 62
4.1 Overall Conditions ... 62
4.2 Temperature Distribution calculations ... 62
4.2.1 Wellbore's Heat Transfer under Seawater ... 62
4.3 Creep Strain of the Material ... 66
4.4 ANSYS simulations ... 69
4.4.1 Total deformation of casing structure ... 69
4.4.2 Elastic Strain Intensity ... 70
4.4.3 Stress Intensity ... 71
4.4.4 Volume changes due to creep deformation ... 72
4.5 Stress Distribution to All Casings ... 73
4.5.1 Meshing, operation to Simulate and Results ... 73
4.6 Sea Water Temperature ... 76

CHAPTER 5: CONCLUSION AND RECOMMENDATION ... 77
5.1 Introduction ... 77
5.2 Conclusion ... 79
5.3 Contribution to Knowledge ... 81
5.4 Future Works ... 81
REFERENCES ... 83
APPENDIX ... 90

LIST OF FIGURES

Figure 1: Typical arrangement of oil well casings 6

Figure 2: Strain-Time graph stages of Creep Deformation in Metals 15

Figure 3: Steady state creep behaviours of the materials 16

Figure 4: Schematic drawing of a typical well design, (A) Structure of an exploration well; (B) Production well (Davies et al., 2014). 18

Figure 5: Schematic drawing of a hydrocarbon well. 19

Figure 6: Routes for fluid leak in cemented wellbore. 19

Figure 7: Scheme of casing centralisation 20

Figure 8: Horizontal wellbore illustration 25

Figure 9 : (A) Well barrier envlop (B) Barrier elements around a well (C) Concept of primary-barrier column and (D) Concept of Secondary barriers. 26

Figure 10: Statistics on casing deformation points of 12 horizontal wells, (Xi et al., 2018). And specific example of Wei-204H7-3 with 5 deformation points as shown by (Yan et al., 2017). 27

Figure 11: 3D view of deformed casing from well (A) non-centralised (B) Centralised (C) Sectional view of simulation (D) Lead mould wash-out from deformed casing. 28

Figure 12: The probability distribution of production casing load and strength (Q. Wang et al., 2018) 28

Figure 13: Challenges of drilling and completion in salt formation (Farmer, Miller, Pieprzak, Rutledge, & Woods, 1996) 30

Figure 14: (A) Casing failure rate in some selected water flowing oilfields (B) Casing failure distribution by stratigraphic formation (Olarte Caro, Marquez, Landinez, & Amaya, 2009). 31

Figure 15: API 5CT Grade J55 Casing Pipe 33

Figure 16: Typical well log signature showing casing deformation (Yin, Deng, et al., 2018; Yin & Gao, 2015; Yin, Han, et al., 2018). 38

Figure 17: (A) Casing imaging logging of an injection well (B) Illustration of shear formation slip inducing casing failure (Yin, Deng, et al., 2018; Yin, Han, et al., 2018; Yin, Xiao, et al., 2018). 39

Figure 18: Pipe Stresses 41

Figure 19: General pipe stresses illustration 42

Figure 20: (A) Riser pipe stack-up and sources of motion (B) Fatigue critical locations (Lim et al., 2012)... 44

Figure 21: Schematic of casing wear (G. Zhang et al., 2011; Q. Zhang et al., 2016)..... 45

Figure 22: (a) Corrosion of tubing (Torbergsen et al., 2012).; (b) Crack in cement (CROOK, KULAKOFSKY, & GRIFFITL, 2003).; (c) Corrosion of casing (Xu, Yang, Li, & Chen, 2006). 46

Figure 23: (A&B) typical example of connection failure. (C&D) presents pin and box thread damage. (Dusseault et al., 2001). 47

Figure 24: (A) Presents a concise summary of casing utilization by well type (B) Casing failure mix by grades on the articles reviewed. (Mohammed et al., 2019).................... 50

Figure 25: Models of well tubular deformation (Pearce et al., 2009). 52

Figure 26: Geometry of the casing 55

Figure 27: Symmetry region of the geometry design of casing structure 56

Figure 28: Meshing 56

Figure 29: Edge sizing (ANSYS).. 57

Figure 30: Body sizing (ANSYS) 57

Figure 31: CAD Model of the casing 58

Figure 32: Geometry Dimensions 58

Figure 33: Mechanical Properties of the material 59

Figure 34: Mechanical Properties of the material (2) 59

Figure 35: Analysis (Static Structural) ANSYS Settings... 60

Figure 36: Thermal conditions 60

Figure 37: Well Structure.. 63

Figure 38: Thermal coefficient along wellnore.. 64

Figure 39: Thermal loss along wellbore.. 66

Figure 40: Creep Strain of the Material 67

Figure 41: Creep Strain model 67

Figure 42: Creep Model 68

Figure 43: Creep Model curve 68

Figure 44: Total deformation (creep analysis) 69

Figure 45: Elastic strain intensity (creep analysis) 70

Figure 46: Stress Intensity (creep analysis) 71

Figure 47: Volumetric changes due to creep deformation (creep analysis) 72

Figure 48: Brick 8 nodes model 73

Figure 49: Casing elongation simulation result (0~51.2m). 74

Figure 50: Casing elongation simulation result (51.2~96.2m) 74

Figure 51: Casing elongation simulation result (96.2~360 m) 75

Figure 52: Casing elongation simulation result (360~1710 m) 75

Figure 53: CAD Model of the casing0 95

LIST OF TABLES

Table 1: Summary of selected casing failure based on well type and operation (Mohammed et al., 2019) 23

Table 2: Chemical composition of API J55 steel [mass. %]. (Sedmak et al., 2020) 33

Table 3: Tensile Properties of API J55 steel. (Sedmak et al., 2020) 34

Table 4: Summary of widely used casing buckling and related buckling model 51

Table 5: Structure Parameters for FEA 54

Table 6: Environmental parameter 63

Table 7: Thermal Injection Parameters 64

Table 8: Temperature distribution to Completion 65

Table 9: Structure parameters of the wellbore 65

Table 10: ANSYS Simulation result summary 69

Table 11: J55 Casing dimensions 90

Table 12: J55 Casing dimensions (2) 91

Table 13: API 5CT Well Casing Length 92

Table 14: API 5CT J55 casing mechanical properties 93

Table 15: J55 Casing tube dimensions 93

Table 16: J55 Casing tube dimensions (2) 94

Table 17: API 5CT J55 Casing tube specifications 94

LIST OF SYMBOLS AND ABBREVIATIONS

API	:	American Petroleum Institute Standards
3D	:	3-Dimentional
ANSYS	:	Computational Analysis Software
O&G	:	Oil and Gas
HPHT	:	High Pressure and High Temperature
BOP	:	Blowout Preventor
MPa	:	Mega Pascal
RQ	:	Research Questions
Cr, Mo	:	Chromium, Molybdenum
FEA, FE	:	Finite Element Analysis, Finite Element
FEM	:	Finite Element Method
DYNTUB	:	Universal 3-D dynamic drill string-in-hole model
CAD	:	Computational Aided Design Software
SAGD	:	Steam Assisted Gravity Drainage
J55	:	Steel type Standard (Casing)
CSS	:	Cyclic Steam Stimulation
ISO	:	International Organization for Standardization
CO_2	:	Carbon Dioxide
$\dot{\varepsilon}_{cr}$	:	Steady State Creep Strain Rate
σ	:	Stress
ID, OD	:	Internal Diameter, Outer Diameter
DOF	:	Degrees of Freedom
LMFBR	:	Liquid Metal Fast Breeder Reactors
HTR	:	Helium Cooled High Temperature Reactors
AGR	:	Advanced Gas Cooled Reactors
LD	:	Linkage disequilibrium

LIST OF APPENDICES

Appendix A: Dimension of Casings…..………………….……………………………... 79

Appendix B: Dimension of Casings (2)……………………….…………………….... 80

Appendix C: Mechanical Properties…...………………………….…...……………... 82

Appendix D: CAD Model of the casing.………….……………………………….... 86

CHAPTER 1: INTRODUCTION

1.1 Background

Creep deformation is a type of plastic deformation that primarily occur in high temperature components. Creep deformation has been studied for many decades primarily in static structures and high operating pipes, tubes etc. Creep is defined as the tendency of solid material to move slowly or deform permanently under influence of persistent mechanical stress. It can occur as a result of long-term exposure to high level of stresses at elevated temperatures. Creep is mostly a concern to engineers and metallurgist when evaluating components that operate in certain high pressure and high temperature environment. Unlike any other deformation, creep deformation does not occur suddenly upon the application of stress. Rather, it is a result and accumulation of a long-term stress.

The goal of this current research is to examine "the Creep Damage Analysis and Numerical Simulation on Oil Well Steel Pipe Casing at Elevated Temperature using Ansys. Creep in structures has been of interest to engineers for more than 200 years. Design of candles was probably one of the first areas where a continuously deforming material under constant load had to be analysed. Examples of other fields where the creep phenomenon has been of importance for the interpretation of the structural response are construction of cable suspended bridges, steam-engine design, power-, chemical-, and petrochemical-plant design, design of jet engines and, nuclear power plant design (Norton, 1929).

Once an oil well has been drilled and reach the reservoir below, the well goes through completion with casings installed in the drilled well to protect and support the well stream. The casing's purpose is to provide stabilisation, and protects the contaminants any fresh water reservoirs from the oil and gas that is being produced. The casing is a fabricated sections or joints that are usually *8m-12m* long and screwed together to form longer lengths of casings called casing strings running down from the production platform to sometimes kilometres beneath the surface to the oil reservoir. As the dept of the reservoir increases, the pressure and temperature increase as well creating high persistent mechanical stresses. This subjects the casings to progressive time-dependent inelastic deformation under mechanical load and elevated temperature, which is defined as Creep.

Creep failure is one of the most important yet complex part when comes to designing. Material Science has defined creep as a tendency of a solid material to undergo through permeant plastic deformation under the influence of high constant mechanical stress and elevated temperatures. These mechanical stresses can be well below the yield strength of the material, however when subjected to prolonged heat and stresses materials experiences permanent plastic deformation. Thus, making creep deformation as one of the complexes yet important part of the designing.

The creep process is accompanied by several different microstructural rearrangements including dislocation, aging of microstructure and grain-boundary cavitation. Hence, a most common grade of casing used by Oil and Gas operators uses is considered in this study. The effects of external and internal mechanical load at elevated temperature unto the casing over time are investigated. The results obtained are then compared for validation of data. This research project uses a numerical approach using ANSYS software in order to simulate various aspects such as the creep model and material damage. The expected results are, that this paper will provide a method to predict high temperature structure lifetime with creep damage, and the effect of creep and fatigue.

As the demand on materials with respect to creep has increased within different applications, theories and methodologies have been developed (Kachanov, 1958). The individual event that probably has had the largest impact on the research and development within the area of creep is the establishment of nuclear power plants such as Liquid Metal

Fast Breeder Reactors, LMFBR, Helium Cooled High Temperature Reactors, HTR, and Advanced Gas Cooled Reactors, AGR (Folke & Odqvist, 1974). Here, the driving force has been the very high safety requirements. In the context of high temperature pressure equipment, the weakening effect of the weldments has been recognized for several decades. In-service inspections have shown that weldments are prone to creep and fatigue damage. It is not uncommon that severely damaged weldments are revealed even before the design life of the component has been reached. In order to improve this situation actions have been taken, both from industry, universities and research institutes, aiming at an enhanced understanding of the weldment response.

However, wellhead uplift was detected during the pilot test among many thermal injection wells. Based on field measuring, the average wellhead uplift is 4~5 cm with the highest reaching 24.5 cm. As the last firewall for oil well safety, Christmas tree should be paid special attention and protected with all kinds of safety precautions the main requirements to casing that provides cementing of oil and gas wells during drilling and operation is their optimum centralisation, which allows achieving a better homogeneity of the slurry flow in the annulus. Optimum standoff between the borehole wall and the casing is ensured with special devices, centralizers put on the casing and spaced along it in a certain pattern. The paper offers a numerical solution to the centralisation of casing. The model includes 3D dynamic equations of the lateral and axial motion of a long pipe in the wellbore with constrained deflections in borehole during tripping operation considering all the major factors typical for casing exploration. A numerical method that enables to determine contact and friction forces as well as standoff between the borehole wall and the casing is proposed (Folke & Odqvist, 1974). Isotropic creep damage models and their applications for crack growth analysis have been shown in this section. These creep damage models generally consist of creep constitutive equation and creep damage evolution equations. According to the difference of damage evolution equations, the creep damage models can be divided into two groups: one is the stress-based creep damage model and the other is the strain-based creep damage model (Norton, 1929).

The stress-based creep damage model has its origin in the attempts by Norton (1929) has been developed with many definitions, containing the models in Sections 2.11. The strain-based creep damage models assume that the damage parameter approaches unity when the local accumulated creep strain reaches a critical creep ductility value, and have also several models for stress-based creep damage models, empirically based creep damage model, such as single empirical mathematical parameter to quantify loss of strength due to numerous mechanisms of degradation. Others models, which are regarded as physically based creep damage model, are developed based on the microstructure damage mechanisms. For a physically based creep damage model, four steps are needed to be implemented: (1) identification of each damage mechanism; (2) definition of a dimensionless damage variable for each mechanism; (3) incorporation of each variable within a constitutive equation for creep; and (4) development of an evolution equation for each variable. For the empirically based creep damage models, there is only one damage variable and no attempt is made to identify the physical nature of the damage parameter and to distinguish between different damage mechanisms. For the physically based creep damage models, to take into consideration of the effects of the different damage mechanisms on creep fracture process, the constitutive equations with single- or multi-damage variable were developed, considering one or more damage mechanisms on the basis of the extent of their application. Summary of isotropic creep damage models and corresponding microstructure damage mechanisms. S. Liu, Zheng, Zhu, and Tong (2014) made a comparison between Kachanov (1958) damage model and Liu-Murakami damage model, and it was shown that the numerical results for Liu-Murakami damage model have a damage delocalisation effect and are relatively insensitive to element size near the crack tip. That means that the Liu-Murakami damage model has significant improvement in damage localisation and the mesh-dependence of the numerical results. These aspects are further argued by C. J. Hyde, Hyde, Sun, and Becker (2010) It is found the Liu and Murakami damage model allows analysis to be performed with more practical time steps and therefore relatively low calculation times. Rouse et, Norton (1929) showed a comparative assessment of hyperbolic sine function model (e.g., Dyson damage model) and power-law based models for use in life prediction. It was indicated that the failure time predicted by Dyson damage model was found to be half the power law models at the lowest stress level and the Dyson damage model was a method to consistently give conservative failure life (T. H. Hyde, Becker, Sun, & Williams, 2006; Norton, 1929).

The assumption of a constant stress exponent in power law models was erroneous due to the possible change in the deformation mechanism. Furthermore, the Dyson model was shown not to be subject to this behaviour due to the use of a sinh function a comparison between Kachanov-Rabotnov damage model and Kowalewski-Hayhurst-Dyson damage model to the stress analysis of thin-walled structures (D. Hayhurst & Webster, 1986a; D. R. Hayhurst, Vakili-Tahami, & Zhou, 2003; R. Hayhurst, Mustata, & Hayhurst, 2005). A good agreement of the numerical results obtained by use of two damage models is obtained for the transient stage at the beginning of the creep process and the difference of the creep strain growth is greater with the further stress relaxation because the sensitivity of the strain rate to the stress levels is approximately the same only for the particular range of stresses used for evaluation of both the damage models (Hore & Ghosh, 2011; Norton, 1929).

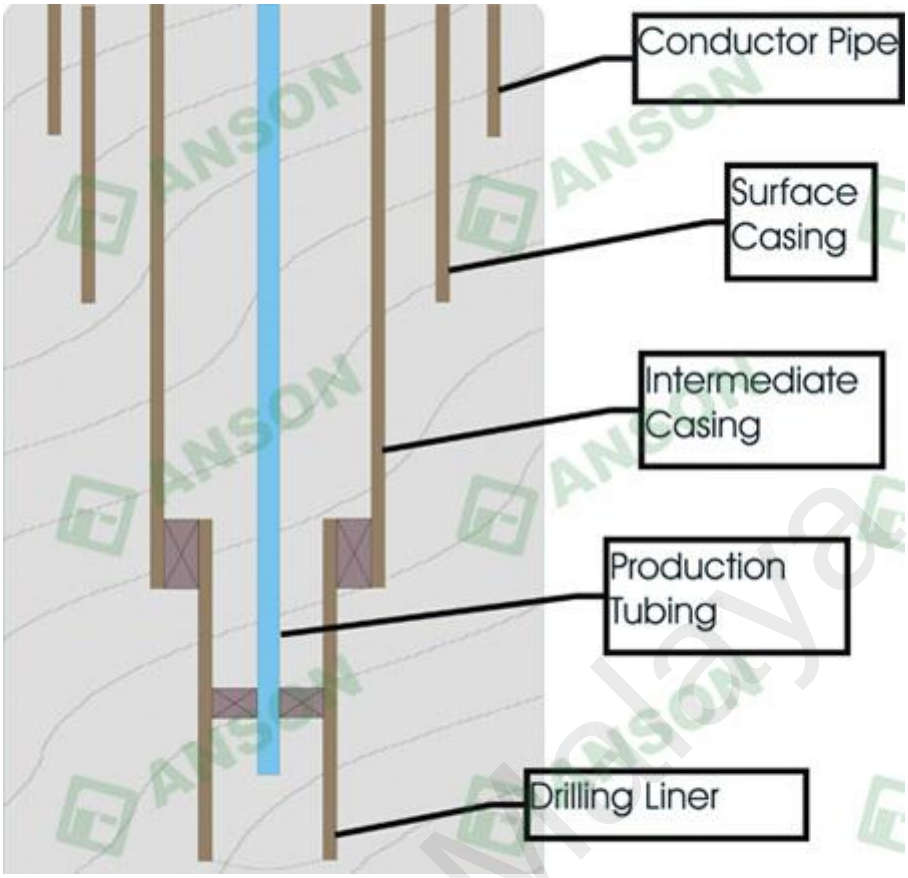

Figure 1: Typical arrangement of oil well casings

1.2 Research Background

Steel casing pipes are used by all Oil and Gas operators as medium to transport crude oil horizontally, Figure 1. While there many grades of production casing pipes used by operator, these steel pipe undergoes tremendous amount of constant pressure and high temperatures. Many studies have been conducted on these extreme pressure's effect to perfect the designing of the production casings, however, studies on the effects of Creep deformation and its long-term effect on these casings are inexplicit.

Replacing these casings can be laborious and costly. As a result, production casings are not frequently replaced or changed throughout the life of the well. This exposes the steel casing pipes to the extreme conditions throughout the life of the well. This study is meant to determine the effects creep damage, but also give the time histories of the element stresses, damage and creep strain. Physical experiment can be costly, time consuming and complex since the production casings can be up to kilometres beneath the surface. Therefore, the conditions will be simulated with ANSYS software to study the behaviours creep.

Major causes of the different grades of casing failures differs on how they behave under long term stress and elevated temperatures. Higher tensile strength casing grades (e.g., P110 & Q125) are mostly used in the deep-water Oil and Gas production. However, P110 candidates record the one of the highest failures owing to its stiffness and high application in injection wells, shale gas, deep-water and High Pressure and High Temperature (HPHT) wells which tends to have a higher failure probability. (Mohammed, Oyeneyin, Atchison, & Njuguna, 2019).

In the beginning of the 1980's, the effect of stress redistribution within the weldment region due to mismatch in creep deformation properties between the weldment constituents was investigated both experimentally and numerically (Nickel, Schubert, Penkalla, & Breitbach, 1991). It was understood that this phenomenon was of importance for the interpretation of the behaviour of the weaker weldments. Based on numerical calculations of the stress and the strain fields, researchers predicted rupture time and rupture position. An initial attempt to define a weldment performance factor was also done. It was defined as that factor by which the pressure had to be reduced to ensure that the welded component attains its design life (Marriott, 1992). The influence of stress state, or degree of constraint, on creep rupture was also recognised thus, not only the stress level but also the characteristic of the stress tensor is essential for the creep rupture process. For a weldment subjected to creep this fact is most essential for the weldment performance (Ivarsson & Sandström, 1980). An enhancement in the degree of constraint also reduces the creep ductility the structural creep response of a weldment obviously becomes very complex as many parameters influence each other another issue that has been focused on since the mid-1980's is seam welded steam pipes in fossil fired power plants. Due to mismatched creep deformation properties between the weld and the parent metal in combination with non-favourable weld shapes, stress concentrations developed within the weldment eventually resulting in seams that fractured catastrophically. Extensive efforts were undertaken which led to the establishment of assessment procedures for this special component. In order to enhance the understanding of the structural creep response of weldments, the continuum damage mechanics concept was introduced as an analyst tool. The possibility to predict creep damage evolution, or evolution of other deteriorating mechanisms, was improved. One obstacle was still, however, the lack of material property data for the weldment constituents(Ivarsson & Sandström, 1980).

Development of the recent shale gas and oil and gas reservoirs sing horizontal wells and recently perfected hydraulic fracturing challenges the structure integrity of the steel casing. Sudden surge and increase in the oil and gas demands have risen the production rates which strains the casings, challenging the designers to handle more failures and how to overcome them. Davies et al. (2014) estimated that some 26,600 wells out of 380,000 wells in Canada, China, Netherlands, Norway, United Kingdom and United States have at least one or more form of structural failures involving oil well casing. On the other hand, Noshi, Noynaert, and Schubert (2018) states that most of these casing failure cases constitutes to about 20 production casings out of 80 production casings examined in the United States and United Kingdom. Furthermore, these casings failure which is caused by the hydraulic fracturing makes up to 85%, in which more than 75% of the failed casings inspected revealed they were damaged due to high hoop stress. (Davies et al., 2014; Noshi et al., 2018).

1.3 Research Problem

Exploration of the Oil and Gas can be very challenging which involves extreme and harsh environments. These conditions challenge the structural integrity of the well's casings. Examples of the some of the harsh conditions the casings are exposed to are such as; deep-water, high temperature, high pressure, and high temperature fields and shale gas. HPHT wells can have bottom hole temperature of at least 150°C with pressure requirement (BOP) that exceeds 10,000psi (69 MPa). Conditions such as these pose a real challenge to the oil well steel casings and expose them to higher chances of leakage. The aim of the major oil producers is have a well construction that is produce Oil and Gas with no leakage, barrier longevity and structurally reliable well integrity throughout the production processes. (Mohammed et al., 2019).

The introduction of the fracture mechanics concept in design and life assessment of high temperature weldments came during the 1990's (D. Hayhurst, 1972; Ivarsson & Sandström, 1980). The research within this field is ongoing and further improvements of current high temperature design codes and life assessment procedures can be expected. Despite the fact that a tremendous amount of work has been spent in understanding the high temperature weldment response, more work remains to be done in order to tackle industry related problems. In-service inspections of high temperature pressure equipment, for example, still show that weldments are prone to creep and fatigue damage. Reasons explaining why this situation prevails are: i) deficiencies in the high temperature design code used; ii) lack of weldment constituent material property data and lack of information about loading conditions at design stage; iii) unfavourable combination of base material and weld deposit material; iv) a welding procedure resulting in unfavourable microstructures across the weldment and introduction of defects; and v) deviation in operation of plant from what was stated in the design specifications. In order to improve the present situation, the very complex behaviour of high temperature weldments has to be further understood. Results from laboratory testing of uniaxial specimens as well as more complex component testing, acquisition of plant experiences in combination with results from numerical simulations should be the basis for this improvement work. The present thesis focuses on numerical simulation of low alloy steel weldments subjected to creep. Both a continuum damage mechanics approach and a fracture mechanics approach are used for a better understanding of weldment performance in high temperature applications (D. Hayhurst, 1972; Ivarsson & Sandström, 1980). The main requirements to casing that provides cementing of oil and gas wells during drilling and operation is their optimum centralisation, which allows achieving a better homogeneity of the slurry flow in the annulus. Optimum standoff between the borehole wall and the casing is ensured with special devices, centralizers put on the casing and spaced along it in a certain pattern. This paper offers a numerical solution to the centralisation of casing.

The research gap that was found in this study is that how the creep deformation actually exists and propagates through the history of the oil well casing. Subsequently, in such cases such as when the creep deformation exists, how does it occur and what causes it. For oil well casing, it is subject to extreme pressure and temperature especially during the fracturing processes and well steam injection processes. Such environmental variables affect the microstructure of the oil well casing and thus advancing to become creep deformation over time. Current studies do not suggest or proves any additional effect of these stresses on the oil well casing materials, even, within the limits of yield strength of the material yet over some period of time and causes irreversible plastic deformation.

1.4 Research Questions

- RQ1 = Jet of complex thermal fluid wounding people when the weld bead of wellhead pipeline cracks due to over uplifting Casing hanger wrecks inside Christmas tree.
- RQ2 = Analysis of Wellhead Uplift in Offshore Thermal Recovery by Using Finite Element Numerical Simulation
- RQ3 = to investigate the Creep Damage Analysis and Numerical Simulation on Oil Well Steel Pipe Casing at Elevated Temperature.

1.5 Research Objective

Once an oil well has been drilled and reach the reservoir below, the well goes through completion with casings installed in the drilled well to protect and support the well stream. The casing's purpose is to provide stabilisation, and protects the contaminants any fresh water reservoirs from the oil and gas that is being produced. The casing is a fabricated sections or joints that are usually *8m-12m* long and screwed together to form longer lengths of casings called casing strings running down from the production platform to sometimes kilometres beneath the surface to the oil reservoir. As the dept of the reservoir increases, the pressure and temperature increase as well creating high persistent mechanical stresses. This subjects the casings to progressive time-dependent inelastic deformation under mechanical load and elevated temperature, which is defined as Creep.

The purpose of this study was to investigate the Creep Damage Analysis and Numerical Simulation on Oil Well Steel Pipe casing at Elevated Temperatures using ANSYS (Computational Structural Analysis). Creep deformation is a type of plastic deformation of solid materials which occurs under high constant stress at high temperatures. Primary purpose of an Oil Well casing is to transport crude oil to the surface as well as separates the fluid or solid of inside the wellbore from the outside environment, whether in solid or in water. Casings of an oil well can experience tremendous pressure change during hydraulic fracturing processes or steam injection processes. The operating loads added with harsh conditions deep beneath the ground or in seawater exerts very high stresses on casings throughout their lifetime Analysis suggest that numerous failures of the casings have been scrutinised, however they only shed minor lights in terms on how these failures occur in terms of the life. Wellhead uplift was detected among some oil wells, and development of offshore thermal recovery technology could be restricted by the serious safety problems behind.

- A numerical approach to investigate and analyse the effect of creep deformation on the oil well steel casing pipe at elevated temperatures.
- To study the strength life and stiffness life of the casing obtain. through maximum damage and maximum creep criterion.

1.6 Research Significance

This research will build the knowledge pool in the area of this paper presents simulation calculation of wellhead uplift-related casing elongation in the air section, seawater section, and strata section by using finite element analysis. Issues are studied including whether the down hole string elongation is uniform, whether the cement between casings is under destruction, and what is the safety limit for uplift.

1.7 Operational Definitions

1.7.1 Creep Damage

Creep damage occurs in metals and alloys after prolonged exposure to stress at elevated temperatures. Creep damage is manifested by the formation and growth of creep voids or cavities within the microstructure of the material (D. Hayhurst, 1972; Ivarsson & Sandström, 1980; Norton, 1929).

1.7.2 Numerical simulation

A numerical simulation is a calculation that is run on a computer following a program that implements a mathematical model for a physical system. Numerical simulations are required to study the behaviour of systems whose mathematical models are too complex to provide analytical solutions, as in most nonlinear systems (Coleman, Parker, & Walters, 1985; Hore & Ghosh, 2011).

1.8 Summary

This chapter has outline research background of the study, problem statement, research question, research objectives and significance of study. In the next chapter, it will review on A theoretical framework is developed to provide a clearer justification of the relationship of those variables the main requirements to casing that provides cementing of oil and gas wells during drilling and operation is their optimum centralisation, which allows achieving a better homogeneity of the slurry flow in the annulus. Optimum standoff between the borehole wall and the casing is ensured with special devices, centralizers put on the casing and spaced along it in a certain pattern.

Studies shows that numerous failures of the casings have been studied, however they only shed minor lights in terms on how these failures occur in terms of the life. Steel casings go through a production life of years sometimes without being replaces or maintained. Concrete casings are also subject to these failures which rarely goes through maintenance or repairs unless required. Primary reason of these is because maintaining or replacing the casing can be extremely expensive. Therefore, the need to perfect the casing's design as well as their ability to handle high pressure and elevated temperature is a mandatory requirement.

The paper offers a numerical solution to the centralisation of casing as well as monitoring the behaviour of API J55 casings creep deformation at elevated stress and temperature. The model includes 3D dynamic equations of the lateral and axial motion of a long pipe in the wellbore with constrained deflections in borehole during tripping operation considering all the major factors typical for casing exploration.

CHAPTER 2: LITERATURE REVIEW

2.1 Introduction

This chapter will discuss the possible reasons that are studied on creep deformation. At a molecular level in metals such as oil well steel pipe casing. The materials subjected to constant pressure at high temperatures experiences a process which is most commonly known as ‘boundary sliding’ deformation. In crystalline solids, creep can form three mechanisms: dislocation creep, diffusional creep, and boundary sliding. These slidings are further divided into two groups which are Rachinger Sliding and Lifshitz Sliding. The adjacent grains or molecular crystals of metals move independently relative to each other, causing the metals to experience Nabarro-Herring Creep with little or no indication of creep formation to individual grains along a fractured edge. In superalloys which are primarily nickel-based, the volume fraction of precipitate particles has a large effect on creep.

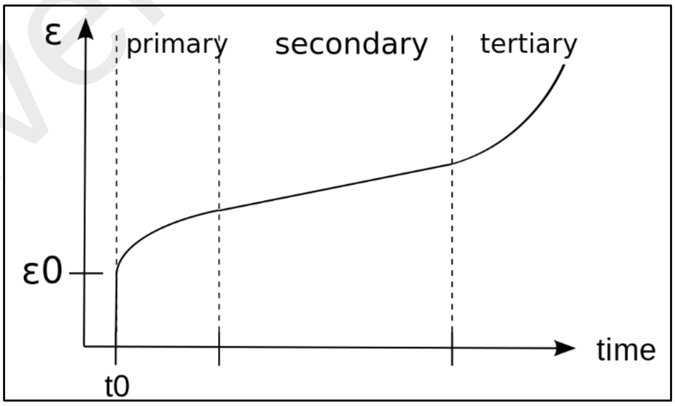

Figure 2: Strain-Time graph stages of Creep Deformation in Metals

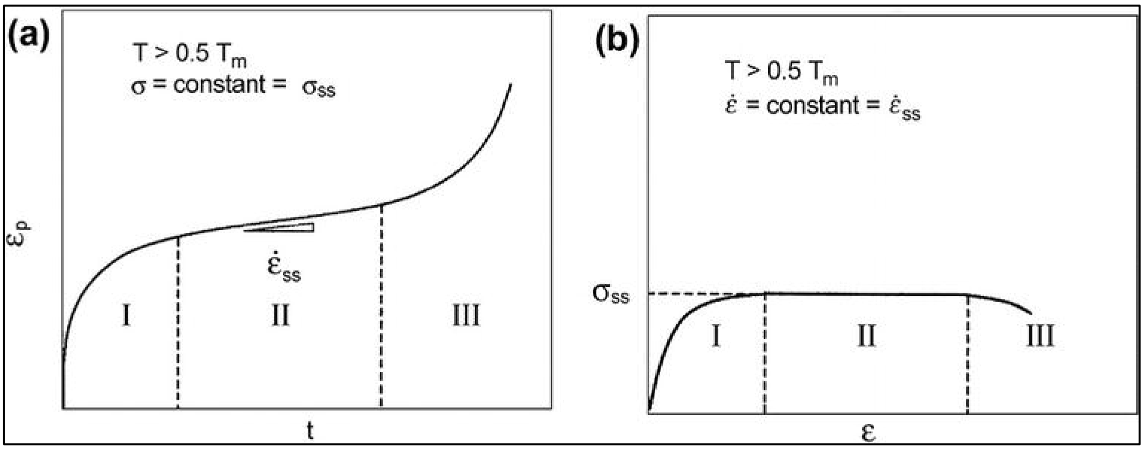

Figure 3: Steady state creep behaviours of the materials

This chapter reviews the factors Creep failure in oil well casings which is also one of the most important failure modes of turbine blade, Figure 2 and Figure 3. Creep is the progressive time-dependent inelastic deformation under mechanical load and high temperature. The creep process is accompanied by many different micro structural rearrangements including dislocation movement, aging of microstructure, and grain-boundary cavitation's. Over the preceding decades, many numerical and experimental investigations have been performed to improve the knowledge of creep of structures under high temperature. Creep constitutive relationship, creep damage evolution equation, and creep life prediction method are three main topics Hayhurst et al. presented a methodology for accurately calibrating constitutive parameters for a 1/2Cr–1/2Mo–1/4V ferritic steel. The accurate description achieved is attributed to the physical basis of the constitutive equations and particularly to the state variables that represents the coarsening of the carbide precipitates and the creep constrained cavity growth Coleman et al. (1985) developed a simple method of estimating material parameters for Dyson-McLean model. Constitutive equations for time independent plasticity and creep of 316 stainless steel at 550° C were given by Hay (Coleman et al., 1985; Hore & Ghosh, 2011). Ma, Shim, and Yoon (2009) presented a method for determining the power law creep constants using the small punch (SP) creep test (Weber & Bendick, 1992). The biggest advantage of SP creep test is that it can be used to evaluate remaining creep life using very small specimens extracted from in-service components. Saad et al. developed a material constitutive model for the P91 and the P92 steels under cyclic loading and high temperature conditions. (Bolton, 2008, 2011) proposed a characteristic-strain model of creep of analysing long term-relaxed stresses and creep strains in engineering components under steady load (Browne, Cane, Parker, & Walters, 1981). Bolton (2008) independently examined the worked example presented in BSI document PD6605-1:1998, to illustrate the selection, validation, and extrapolation of a creep rupture model using statistical analysis (Browne et al., 1981). Wilshire and Scharning (2008) presented a new approach to analysis of stress rupture data allowing rationalization, extrapolation, and interpretation of multipitch creep life measurements reported for ferritic 1Cr– 0.5 Mo tube steel Holdsworth et al. reviewed results are of an ECCC work program to investigate procedures for the practical representation of mean creep behaviour for well specified alloys from large multisource, multicast strain-time datasets. Leinster (2008) proposed a method of creep rupture data extrapolation based on physical processes. G. Zhang et al. (2011) studied creep-fatigue interaction damage evolution of the nuclear engineering materials modified 9Cr– 1Mo steel with continuum damage mechanics (CDM) theory.

Wilshire and Burt (2008) interpreted normal creep curves in terms of the deformation mechanisms controlling strain accumulation and the damage processes causing tertiary acceleration and eventual failure. T. H. Hyde et al. (2006) used single-state variable and three-state variable creep damage constitutive models to investigate the material behaviour of two P91 steels of differing strength. Spindler determined the material properties of some creep and constant strain rate tests on a Type 347 weld metal, and then various creep damage models are used to predict the creep damage in some creep-fatigue tests on the same Type 347 weld metal. Guan, Xu, and Wang (2005) presented quantitative study of creep cavity area of HP40 furnace tubes. C. J. Hyde et al. (2010)

presented a novel modelling process for creep crack growth prediction of a 316 stainless steel using continuum damage mechanics, in conjunction with finite element (FE) analysis Smith et al. investigated the type IV creep cavity accumulation and failure in steel welds (Browne et al., 1981). The main requirements to casing that provides cementing of oil and gas wells during drilling and operation is their optimum centralisation, which allows achieving a better homogeneity of the slurry flow in the annulus. Optimum standoff between the borehole wall and the casing is ensured with special devices, centralizers put on the casing and spaced along it in a certain pattern (Browne et al., 1981; Viswanathan, 1989). The paper offers a numerical solution to the centralisation of casing, Figure 4, Figure 5, Figure 6.

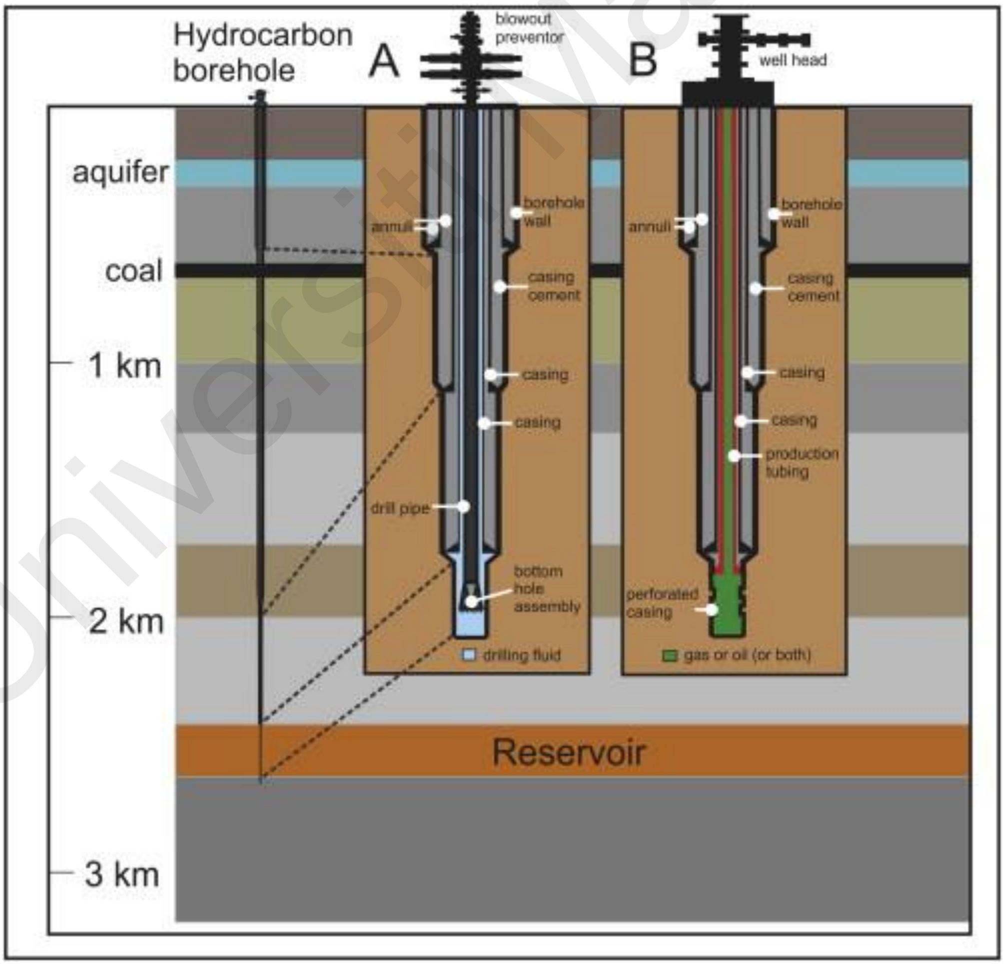

Figure 4: Schematic drawing of a typical well design, (A) Structure of an exploration well; (B) Production well (Davies et al., 2014).

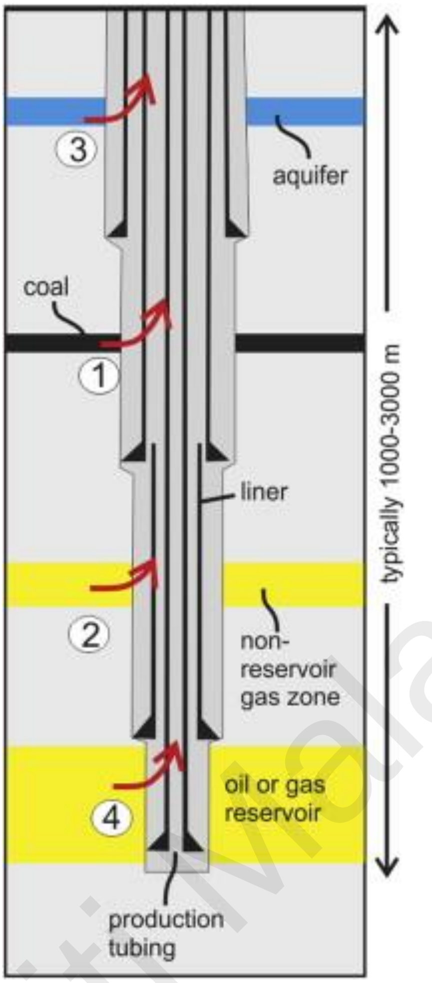

Figure 5: Schematic drawing of a hydrocarbon well.

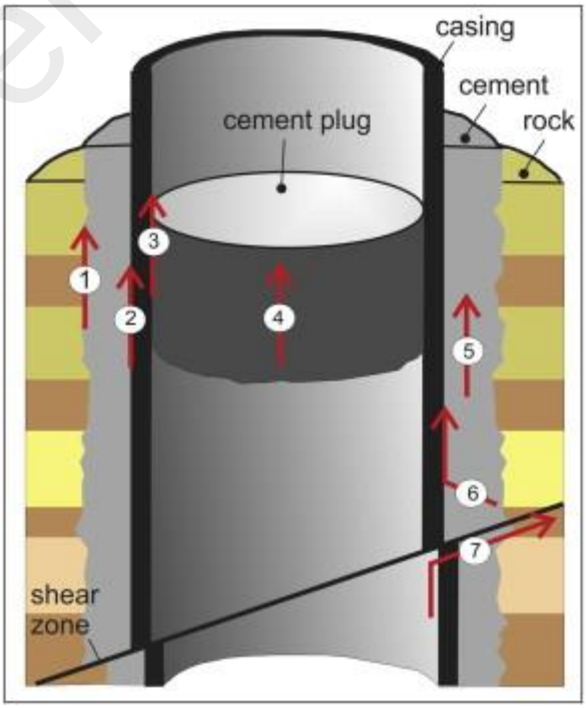

Figure 6: Routes for fluid leak in cemented wellbore.

2.2 Numerical Simulation of Casing Centralisation

One of the main requirements to casing that provides cementing of oil and gas wells during drilling and operation is their optimum centralisation, which allows achieving a better homogeneity of the slurry flow in the annulus Figure 7.

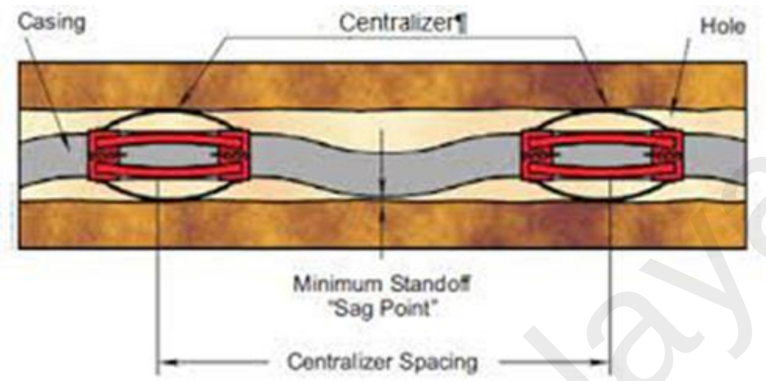

Figure 7: Scheme of casing centralisation

It appropriate to recall about the recent Macondo disaster (Williams, Coleman, & Walters, 1984) when BP responsible for well cementing miscalculated about the number of centralisers. This resulted in inadmissible reduction of standoff between the borehole wall and the casing in some sections preventing homogeneous flow of cement slurry in the annulus required for its filling and integrity. Finally, drilling mud was left in the standoff that could not prevent oil and gas travel up the well. There are two types of centralisers: rigid and flexible (bow-spring) ones. Rigid centralisers can be considered as bulges on the drill pipe body or BHA in the form of tool joints or stabilisers. Contact and friction forces as well standoff between the borehole wall and the casing for such centralisers can be calculated based on the drill string contact model using the FEM or the finite difference method. Methods of calculation the standoff between the borehole wall and the casing body for bow-spring centralizes are described in specification. Unfortunately, the model used in the above paper does not account for elastic deflection of centralisers, which can result in the standoff underestimation for wells with substantial variation of hole size and high tortuosity. In paper a serious step was made towards improvement a conventional model, however, it also requires further refinement of the model of contact forces acting on the casing with the varying diameter as well as improvement of the numerical method for solution of a contact problem. This paper offers a numerical solution to the centralisation of casing. Isotropic creep damage models and their applications for crack growth analysis have been shown in this section. These creep damage models generally consist of creep constitutive equation and creep damage evolution equations. According to the difference of damage evolution equations, the creep damage models can be divided into two groups: one is the stress-based creep damage model and the other is the strain-based creep damage model. The stress-based creep damage model has its origin in the attempts by Kachanov and Rabotnov, and has been developed with many definitions, containing the models in sections below (Kachanov, 1958). The strain-based creep damage models assume that the damage parameter approaches unity when the local accumulated creep strain reaches a critical creep ductility value, and have also several models e.g., (Smith, Walker, & Kimmins, 2003; Spindler, 2005; Webster & Ainsworth, 2013) damage model. For stress-based creep damage models, empirically based creep damage model, such as Kachanov-Rabotnov damage model and Liu-Murakami damage model, is obtained by defining a single empirical mathematical parameter to quantify loss of strength due to numerous mechanisms of degradation. Others models, which are regarded as physically based creep damage model, are developed based on the microstructure damage mechanisms. For a physically based creep damage model, four steps are needed to be implemented: (1) identification of each damage mechanism; (2) definition of a dimensionless damage variable for each mechanism; (3) incorporation of each variable within a constitutive equation for creep; and (4) development of an evolution equation for each variable.

The main requirements to casing that provides cementing of oil and gas wells during drilling and operation is their optimum centralisation, which allows achieving a better homogeneity of the slurry flow in the annulus. Optimum standoff between the borehole wall and the casing is ensured with special devices, centralizers put on the casing and spaced along it in a certain pattern. The paper offers a numerical solution to the centralisation of casing. The model includes 3D dynamic equations of the lateral and axial motion of a long pipe in the wellbore with constrained deflections in borehole during tripping operation considering all the major factors typical for casing exploration. A numerical method that enables to determine contact and friction forces as well as standoff between the borehole wall and the casing is proposed It is found the Liu and Murakami damage model allows analysis to be performed with more practical time steps and therefore relatively low calculation times comparative assessment of hyperbolic sine function model (e.g., Dyson damage model) and power-law based models (e.g., Kachanov-Robotnov and Liu-Murakami damage model) for use in life prediction. It was indicated that the failure time predicted by Dyson damage model was found to be half the power law models at the lowest stress level and the Dyson damage model was a method to consistently give conservative failure life (C. J. Hyde et al., 2010). As what we have discussed in chapter one of this paper, the assumption of a constant stress exponent in power law models was erroneous due to the possible change in the deformation mechanism. Furthermore, the Dyson model was shown not to be subject to this behavior due to the use of a sinh function. (T. H. Hyde et al., 2006; Kachanov, 1958) made a comparison between Kachanov-Rabotnov damage model and Kowalewski-Hayhurst-Dyson damage model to the stress analysis of thin-walled structures.

A good agreement of the numerical results obtained by use of two damage models is obtained for the transient stage at the beginning of the creep process and the difference of the creep strain growth is greater with the further stress relaxation because the sensitivity of the strain rate to the stress levels is approximately the same only for the particular range of stresses used for evaluation of both the damage models. The hyperbolic function in

Kowalewski-Hayhurst-Dyson damage model gives more adequate stress level dependence for wide stress ranges as power law function in Kachanov-Rabotnov damage model (D. Hayhurst, 1972; D. Hayhurst & Webster, 1986b). The model considers 3D dynamic equations of the lateral and axial motion of a long string in the well with constrained deflections in wellbore considering all the major factors typical of casing exploration. This model represents a further development of multi-functional DYNTUB model, previously designed for the dynamic simulation of tubular in 3D wellbore during drilling with rotation and without rotation, tripping operation, buckling and whirling of drill string, etc. Examples of standoff ratio calculations for casings of varying sizes and wells with different inclination and tortuosity are presented (Williams et al., 1984).

2.3 Casing integrity challenge in different well types

The Oil and Gas wells can be further categorised as conventional and unconventional wells. Primary difference between the two types is that unconventional resources or wells are not conventionally developed. Unconventional wells can include extreme depths, elevated stress, high bottom hole temperature as well as presence of greenhouse gasses. Therefore, these unconventional wells also subject the oil well casings to abnormal and high stresses and temperatures which brings the probability of failures to a much higher level.

Table 1: Summary of selected casing failure based on well type and operation (Mohammed et al., 2019)

Well/Operation	Major Cause of Failure/Reasons
Vertical/Water flooding	Formation slippage
Producers and injectors/water flooding	Water flooding effect and pressure differentials, high value of injection pressure, asymmetric distribution fractures, both natural fracture and induced fractures and Poor-quality cementing ring.

Deviated/drilling and completion	Violent string contact/Wear and corrosion. Dog-leg and large pressure fluctuations during fracturing
Vertical/steam flooding	Large thermal stresses, in situ combustion, fatigue, steam leak leading to formation slip and thermo-chemical mechanical loads.
Vertical/SAGD and CSS	Thermally induced strain based cyclic axial loading and net internal & external pressure differentials.
Horizontal well/Hydraulic Fracturing	Fault slip, unequal in-situ stress field, degree and stress deficit areas - increased the shear effect to increase, and the radial ellipse deformation and axial S-shaped deformation of casing to increase at the same time. Fatigue coupled thermal-mechanical effect, shear, leap, and slip around the casing String. Natural fractures and faults increase failure probability. Shear deformation induced by the slip of shear fractures.
Vertical/Drilling, completion and production	Collapse pressure from salt rock creep, annulus pressure build-up owing to fluid thermal expansion in sealed annuli.
Deviated/perforations	High perforations density and reservoir compaction
Deviated/cyclic steam stimulation	Extra plastic deformation under tension and compression loads during thermal stimulation.
Vertical/Production and depletion	Inclination and reservoir compaction/depletion.
Others	Unequal in situ stress, non-uniform external pressure, fatigue crack nucleation, Wear, well closure and instability due to creep, drawdown/compaction and corrosion.

2.3.1 HPHT & geothermal wells

In HPHT and Geothermal wells, the average hole temperature ranges from 232° to 400° C. These kinds of high pressure and high temperature well is found in location of high thermal gradient which is above than the world's average thermal gradient (e.g., 1.4° F/100ft). Due to such elevated temperature and pressure of the well, the casings and cement are subjected to abnormal and subnormal pressure zones during the drilling stages as well as the production stage. Due to these, both pressure zones creates alternating pressure sequence and pose extreme or harsh conditions to both casings and cement structure of the oil well. Long term exposure to these conditions can accelerate corrosion as well as failures – such as collapse and burst.

2.3.2 Shale gas horizontal wells

Oil well such as shale gas and horizontal wells naturally exhibits low permeability. Therefore, suggesting these types of wells require an additional stimulation aid for the hydraulic fracturing process during the drilling stages. The horizontal wells are a very long horizontal lateral section which during the hydraulic fracturing process, the temperature drops at a very fast rate, added with a high flow rate, this temperature plunge causes uneven load distribution on the casing. Resulting in more chances of having a deformation.

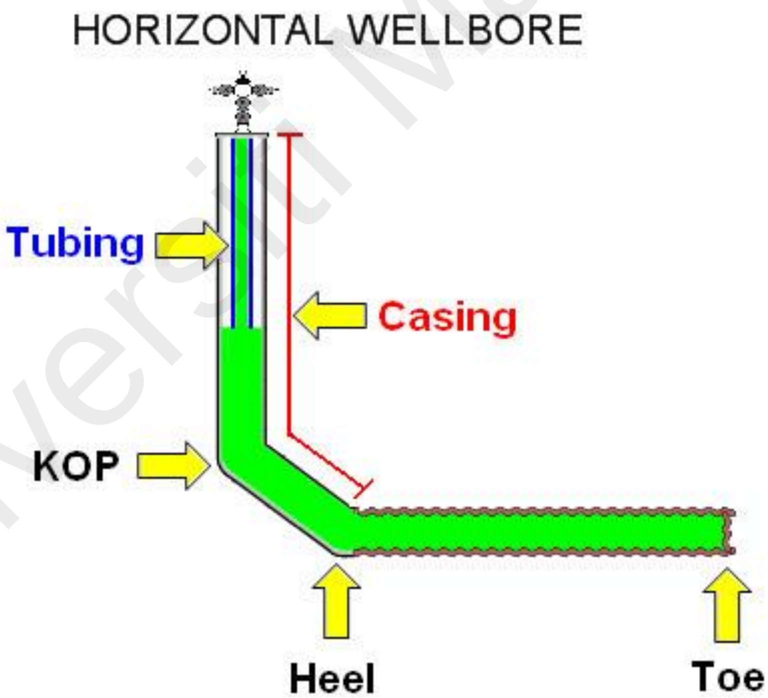

Figure 8: Horizontal wellbore illustration

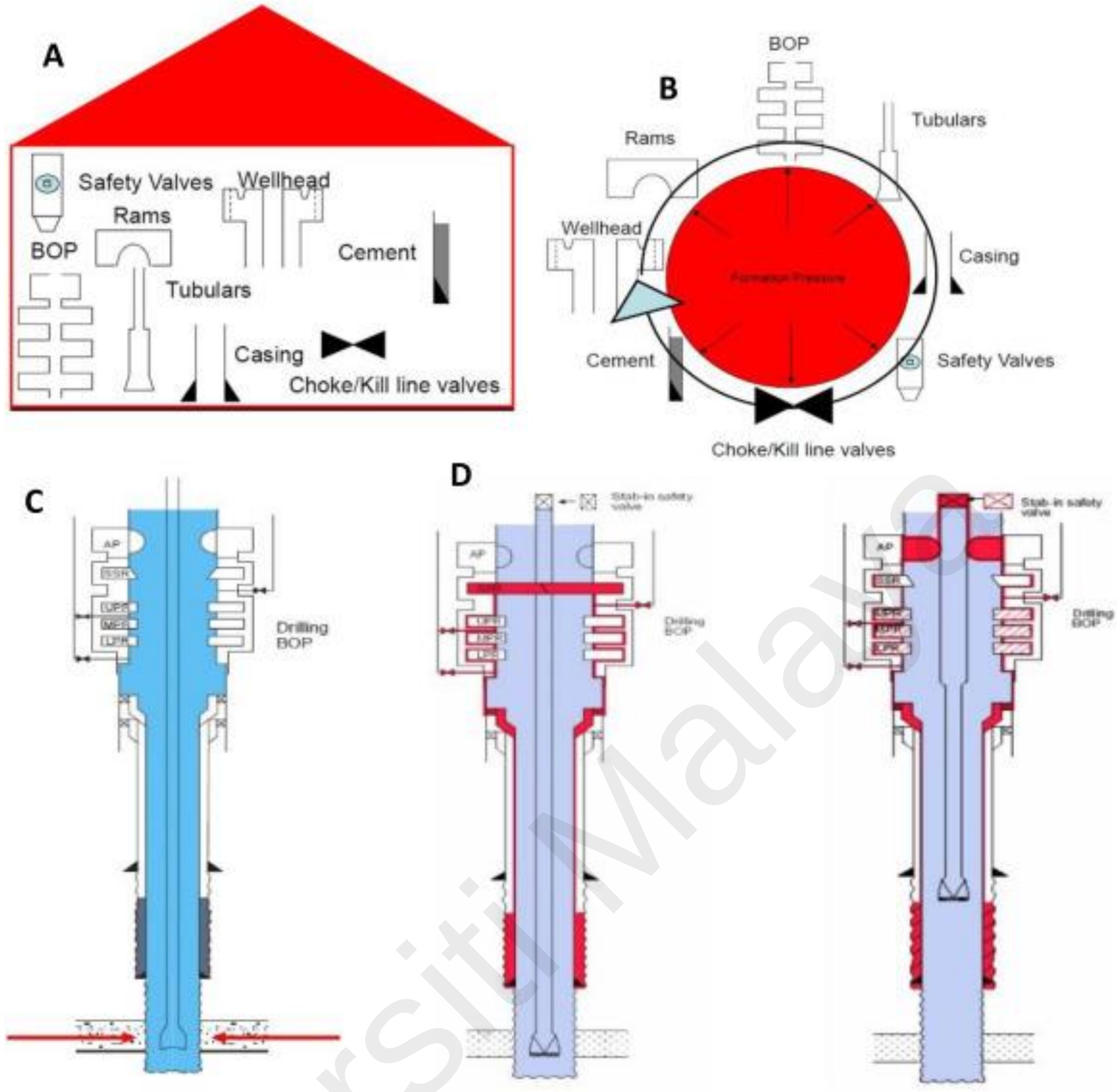

Figure 9 : (A) Well barrier envlop (B) Barrier elements around a well (C) Concept of primary-barrier column and (D) Concept of Secondary barriers.

In general, hydraulic fracturing is the biggest factor in terms of causing deformation to the casings. Fracturing processes causes structural stresses that lead to wellbore integrity decline (Davies et al., 2014; Mohammed et al., 2019). Both Q. Wang, Zhang, and Hu (2018) and Xi, Li, Liu, Cha, and Fu (2018) mentions that additional load and stresses are experienced by the casing during the fracturing processes which results in casing damage under the action of formation shear slip. Both pointed out that fracture slip during hydraulic fracturing can cause shear slip, Figure 8, Figure 9.

The research conducted by Xi et al. (2018) shows that the casing stress increases primarily due to formation anisotropy, lithologic interface, temperature and cement. Statistically showing that deformation points of 12 wells our of 25 horizontal wells during hydraulic fracturing. It could be deduced that different category of casing deformations were encountered during fracturing, tripping bridge and those related to drilling out the bridge plug Figure 10, Figure 11.

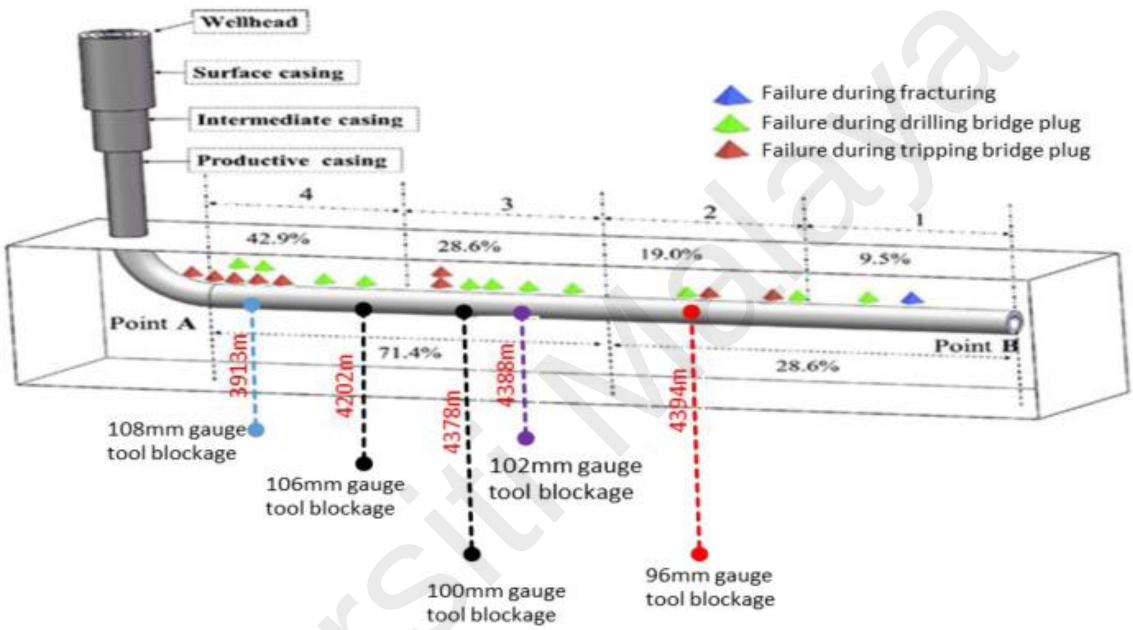

Figure 10: Statistics on casing deformation points of 12 horizontal wells, (Xi et al., 2018). And specific example of Wei-204H7-3 with 5 deformation points as shown by (Yan et al., 2017).

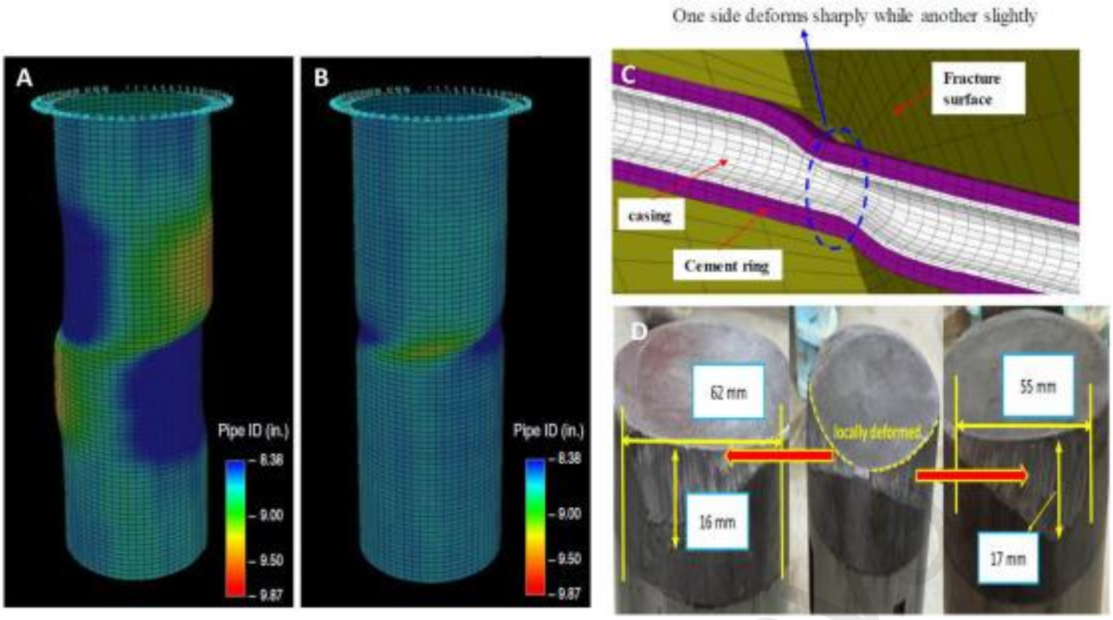

Figure 11: 3D view of deformed casing from well (A) non-centralised (B) Centralised (C) Sectional view of simulation (D) Lead mould wash-out from deformed casing.

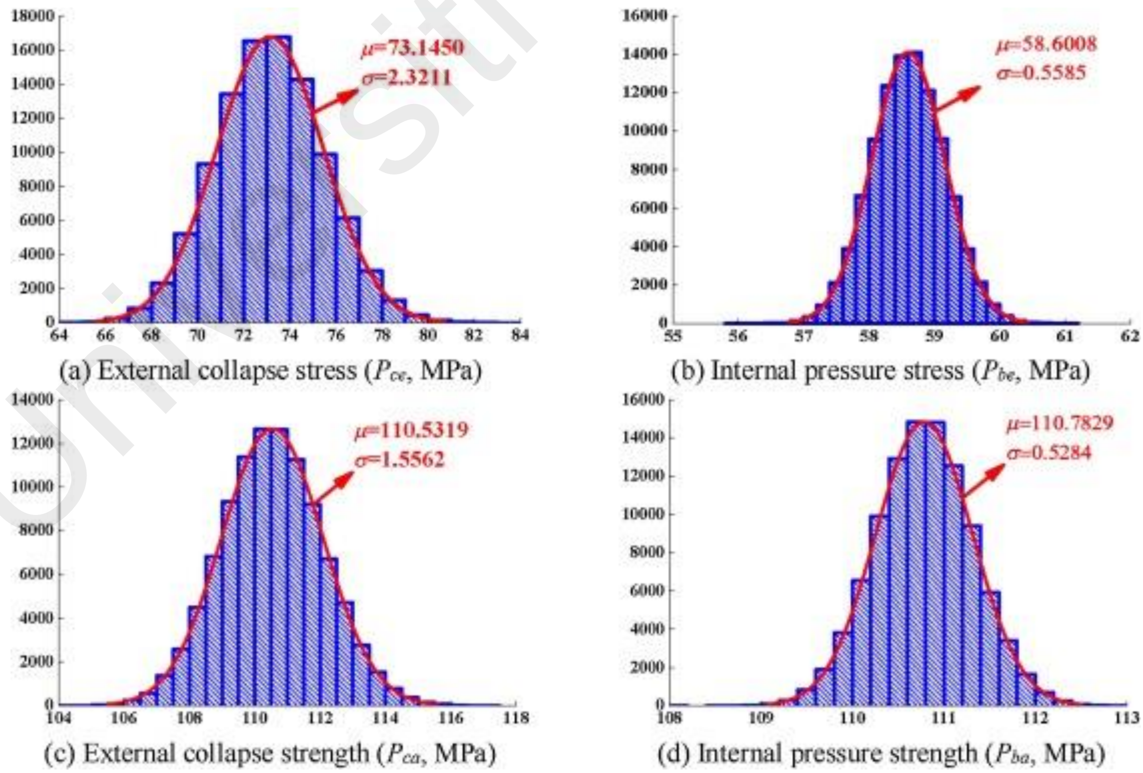

Figure 12: The probability distribution of production casing load and strength (Q. Wang et al., 2018).

2.3.3 Deepwater wells

In oil and gas context Deepwater wells are referred to as wells which are more than 1,000 feet in water depth and ultra-deep wells which refer to wells that are beyond 5,000 feet of depth. This new depth brings new and unique challenges to the casing strength integrity. H. Wang and Samuel (2016) mentions that during exploration, huge accumulation of hydrocarbon is found in deep-water typically below salt formations. As a result, processes such as drilling, completion, and production poses great challenges and risky and expensive to well travers salt formations. Additionally, salt formations flow plastically under creep to close the wellbore. As a result, creep deformation occurs more than often during the exploration of Oil and Gas. In China to mention a few, casing failure problems due to uneven external salt loading are often frequent which causes a major impact on the economic losses. (Zhao, Chen, & Wang, 2011). A study conducted by H. Wang and Samuel (2016) related casing deformation to Salt creep rate and casing temperature conditions. Further research in this fields indicates that the effect of temperature on a particular well in Gulf of Mexico justifies salt temperature of 48° C and the bottom of base salt at 93° C accelerated the creep rate at the bottom to about 100 times faster primarily due to temperature difference. This shows, increase in temperature magnifies the tangential stress of cement sheath resulting in increase in compressive stress on the casing, hence improving the chances of buckling to occur (Dusseault, Maury, Sanfilippo, & Santarelli, 2004; Fan, Deng, Tan, & Liu, 2018). Figure 13.

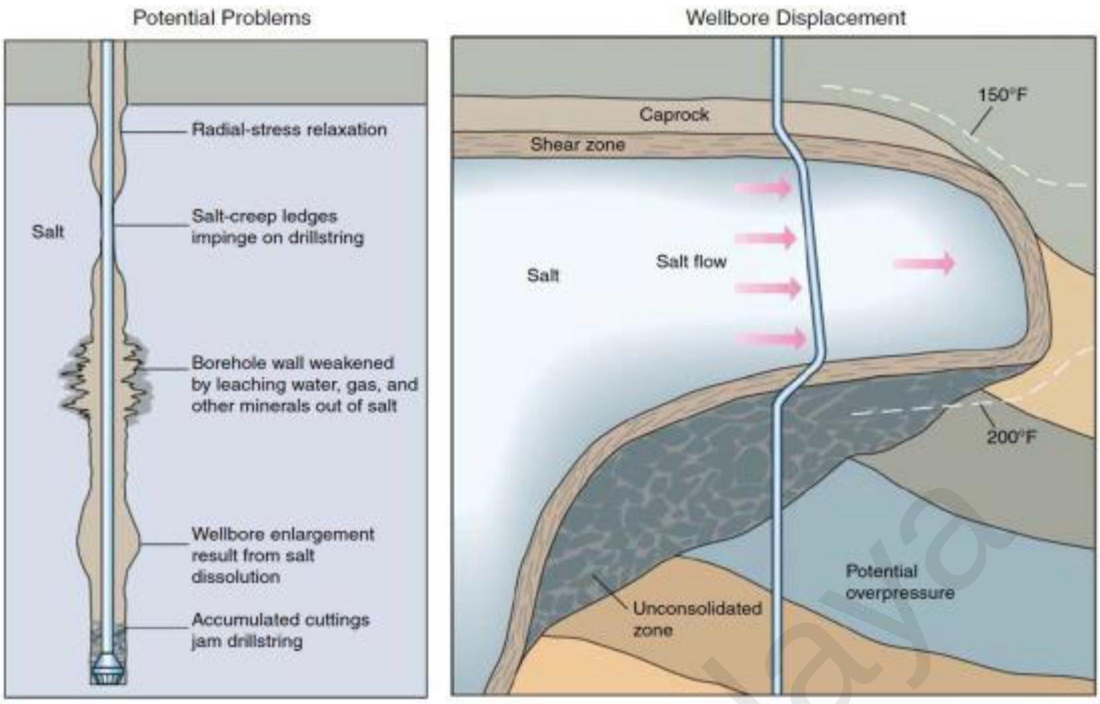

Figure 13: Challenges of drilling and completion in salt formation (Farmer, Miller, Pieprzak, Rutledge, & Woods, 1996).

2.3.4 Injection wells

Injection wells uses a technique which is called water flowing to recover the oil and gas from the reservoir once the reservoir drive mechanism declines. Using this technique, injection wells are drilled or producing well may be converted to injector depending on the injection patters and optimum sweep efficiency. Based on the studies conducted, formation of slippage was identified as the main cause of the casing's failure. Hence affecting the longevity of wells and reducing the economic benefit of oilfields. As an example, 72% of production wells and 63% of injection wells have some sort of casing failures (Yin, Deng, He, Gao, & Hou, 2018; Yin & Gao, 2015; Yin, Han, et al., 2018; Yin, Xiao, Han, & Wu, 2018).

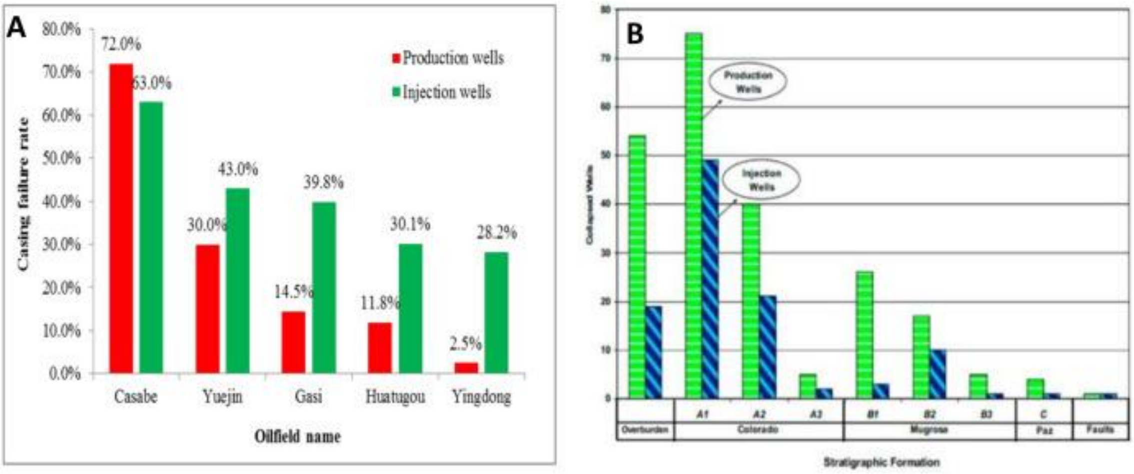

Figure 14: (A) Casing failure rate in some selected water flowing oilfields (B) Casing failure distribution by stratigraphic formation (Olarte Caro, Marquez, Landinez, & Amaya, 2009).

As shown in the Figure (B) in Figure 14 including the casing failure distribution relative to stratigraphic formation. Injection formation and overburden formation is where casing failures or deformation mostly occur. This indicates, the additional load on the casing which caused the failure is mainly caused injection that induces the formation deformation (Yin, Han, et al., 2018).

2.3.5 Steam injection for heave oil recovery

Steam injection is also called as thermal recovery. Widely used in countries such as Canada and Venezuela, where they have abundant heavy oil and sands resources. This method constitutes to variation of cyclic steam stimulation (CSS), steam flood or steam assisted gravity drainage – SAGD (K. Guo, Li, & Yu, 2016). The purpose of the steam injection into the well is to increase the production efficiency. However, this process reduces the crude oil viscosity, which is to facilitate he oil production but induces additional thermal stress to production casing during the process. Thermal cyclic loads causes the casing to expose to more casing buckling and formation shear movements (J. Wu & Knauss, 2006). During the steam injection processes, large amount of volumetric changes occur within the casing. Changes such as high temperature, convective heat transfer and contraction puts an additional strain on the casing structure. The net effect of this volumetric changes produces a net effect on entire structural deformity of both cement casing and surrounding formation. According to the statistics, numerous thermal recovery well casing failure occurred around the world, which makes the wellbore to lose integrity, lost production and additional costs incurred (Xie & Liu, 2008). Injection well can have an average temperature of 221° C to 350° C, whereby the casing failures occur due to high pressure and high temperature caused by the injection steam. As a result, the stresses often exceed elastic limit of typical thermal well casing materials causing the failures. Additionally, cyclic stresses which is repeated throughout the oil and gas production affects severely the well mechanical response leading to well integrity issue (Ichim, Marquez, & Teodoriu, 2016; Ichim & Teodoriu, 2016).

2.3.6 Choosing J55 Standard oil well steel casing pipe.

J55 casing tube is a steel tube used for supporting the wall of petroleum and gas wells so as to ensure that the well is operating normally during and after the drilling process. Each oil well would need several layers of casings according to different drilling depth and geological conditions. J55 oil well casing pipe is an important tool used in oil drilling. It has excellent elongation property. After the pipe is in the well, the well is then be cemented. Unlike oil pipe and drill rod, casing tube is not reusable. Therefore, casing pipe consumption occupies more than 70% of the whole oil well pipes.

Figure 15: API 5CT Grade J55 Casing Pipe

2.3.6.1 Applications

API J55 casing tube is widely used in the foundation works of many industries, such as petroleum, natural gas, coal gas, water supply, thermal power generation, hydropower generation, dredging engineering, etc. Figure 15.

2.3.6.2 Properties

The J55 casing tube is cooled after tempering process. This method helps the pipe avoid the high-temperature brittleness and gain toughness. Subcritical quenching method is adopted to effectively reduce harmful elements and impurities.

- Casing tube of J55 steel grade is strong, durable and reliable.
- This oil well casing pipe has sturdy construction.
- Economic rate of return is very high.
- This product is water and leak proof.
- This casing tube is light in weight.

Table 2: Chemical composition of API J55 steel [mass. %]. (Sedmak et al., 2020)

C	Si	Mn	P	S	Cr	Ni	Mo	V	Cu	Al	C_{eq}

0.29	0.23	0.96	0.013	0.022	0.1	0.058	0.012	0.003	0.13	0.025	0.49

Table 3: Tensile Properties of API J55 steel. (Sedmak et al., 2020)

Specimen	Temperature	Yield strength	Ultimate tensile strength	Elongation
	[°C]	R_{eH} [MPa]	R_m [MPa]	A [%]
1	20	376	559	33.5
2		384	566	31.4
3		379	562	34.2
Mean value		379.7	562.3	33
Standard API 5CT		379–552	>517	>22.5

2.4 Current Advances

Numerical simulation calculation is a widely applied research method both domestic and overseas in analysing casing stress and deformation process during thermal injection and production. According to the investigation, the numerical study on the stress state and deformation process of casing is less abroad. The finite element method is used to analyse the wellbore, casing, and formation as whole and to establish the wellbore and formation temperature field calculation model at home. Under ideal conditions, the bearing characteristics are analysed under the action of uniform internal pressure, uniform ground stress, and temperature load. The method does not consider the casing state of different sections, and the error is larger. Now, domestic application of finite element analysis is operated in steps. First, take wellbore, casings, and strata as an entity and build a temperature calculation model. Then, build a stress field calculation model and analyse the stress status of steam injection string and the casing string in the well. Obtain stress and strain of casing string by deriving stress calculation formats of steam injection string and casing string while operating. Furthermore, based on the ideal conditions of uniform internal pressure, uniform stress, and uniform temperature load, analyse the bearing behaviour of the selected study object of casing-cement sheath-strata with plane strain element PLANE183. Although there is a lot of analysis on casing stress, wreck, and precautions for thermal recovery both domestic and overseas, still no integrated solution for wellhead uplift is brought up. Exploratory research on wellbore uplift in offshore thermal recovery is also under its way, most of which bases on the ideal cylinder model without casing coupling. Besides, the uplift calculation is mainly based on free elongation, which cannot accurately simulate the real structure and uplift process of thermal recovery wellbores. Limitations of existing calculation methods are as follows Temperature field plays a decisive role in casing elongation and Christmas tree uplift. However, in present calculations for temperature field, seawater's impact on heat transfer is neglected. In fact, considering the differences between land recovery and offshore recovery, seawater has a major influence on temperature distribution to the three layers of casings. In present domestic research, downhole string is always taken as an entity under uniform load and applied plane strain element, while, in this paper, 3D finite element model is built for simulation, which is unlike the present model without decoupling and sliding between casings, cement sheath, and strata. By simulating the casing stress and elongation separately in the air section, seawater section, and strata section, the new model makes sure the simulation conditions are more congruous with real work conditions and leads to more accurate result (Williams et al., 1984).

2.5 Creep Damage Analysis and Numerical Simulation on oil well steel pipe

One of the main requirements to casing that provides cementing of oil and gas wells during drilling and operation is their optimum centralisation, which allows achieving a better homogeneity of the slurry flow in the annulus. Optimum standoff between the borehole wall and the casing is ensured with special devices, centralisers put on the casing and spaced along it in a certain pattern. This paper offers a numerical solution to the centralisation of casing. The model includes 3D dynamic equations of the lateral and axial motion of a long pipe in the wellbore with constrained deflections in borehole during tripping operation considering all the major factors typical for casing exploration. A numerical method that enables to determine contact and friction forces as well as standoff between the borehole wall and the casing is proposed. Examples of standoff ratio calculations for casings of varying sizes and wells with different inclination and tortuosity are presented. The most commonly used welding technique in high temperature applications is manual metal arc welding. A characteristic weld contains several beads and has a weld width that increases towards the outer surface of the component. The microstructure developed during welding will vary across the weldment as well as within the beads. What type of microstructure that is developed is essentially controlled by the heat cycle the material experiences and the characteristics of the material, i.e., chemical composition, microstructure before welding (base material), etc. A subsequent post weld heat treatment reduces residual stresses introduced during welding as well as influences the mechanical properties of the weldment constituents (D. Hayhurst & Webster, 1986a; R. Hayhurst et al., 2005). Isotropic creep damage models and their applications for crack growth analysis have been shown in this section. These creep damage models generally consist of creep constitutive equation and creep damage evolution equations. According to the difference of damage evolution equations, the creep damage models can be divided into two groups: one is the stress based creep damage model and the other is the strain-based creep damage model The stress-based creep damage model has its origin in the attempts and has been developed with many definitions, the strain-based creep damage models assume that the damage parameter approaches unity when the local accumulated creep strain reaches a critical creep ductility value, and have also several models e.g. Nikbin-Smith-Webster, Spindler and Wen-Tu damage model (Nickel et al., 1991; Smith et al., 2003; Weber & Bendick, 1992).

2.6 Overview of failure modes

As discussed in chapters before, existing and induced downhole stresses in conventional and unconventional subjects the well and well casing into several challenges, especially to casing integrity throughout well life cycle. Multiple factors affect the casing's failure which are well location, bore hole temperature, volumetric flow, reservoir characteristics and regional geo-stress distribution. Depending on the variation of the stresses and degree of rock consolidation and strength – wellbore instability issues could occur during the drilling stages. Radial and tangential stresses are critical to borehole stability, additionally, tangential (hoop) stress variation in horizontal wells is even worse and undoubtedly can cause casing plastic deformation. Studies also showed that, differences in moduli can cause significance variation in stresses along radial and tangential directions, this is because the material non-linearity between the casing and the cement. At cement – casing interface, moduli variation can affect casing collapse resistance by up to 10% (Kiran et al., 2017).

2.6.1 Buckling failure or deformation

This section will discuss one of the failure modes of the casing which is by buckling and specific factors causing casing lateral buckling and the failure mechanism. In summary, there are two main types of buckling of casing in horizontal well which are sinusoidal and helical. Axial compression load gives rise to sinusoidal buckling configuration, however these conditions depends on casing stiffness, weight and hole size (Zhanfeng Chen, Zhu, & Di, 2018). Researchers pointed out that shear stresses and local stresses of weak formation are the primary causes of casing deformation mechanism (Dusseault, Bruno, & Barrera, 2001; W. Liu, Yu, & Deng, 2017). Primary factors of the buckling failure of casing buckling are due to increased axial loading, caused by combined effect of perforation and huge volume of acid treatments. As a result, these factor lead to big vertical cavities and poor radial constraints of the casing (Furui, Fuh, Abdelmalek, & Morita, 2010). Furthermore, other reasons such as increase in pumping rates, a critical value is reached which cause natural fracture leading to casing lateral deformation. Zhaowei Chen, Shi, and Xiang (2017) states that at some critical pressure, natural fracture is activated which move and induce casing failure. During the stages of drilling, the rock removal creates an imbalanced load and strain, thus causing overburden and horizontal stresses onto the well. To add to this, wellbore stability issues manifest which them leads to a buckled casing. Moreover, during the fracturing processes, casing failure is also recorded which are due to slip of bedding planes and natural fracture caused by uneven loads. On the other hand, displacement that occurs due to dip angle or various strata also gives an upper hand to buckling failure. Each of these faults develops unique casing buckling failure in the well (Y. Guo, Blanford, & Candella, 2015; Xi et al., 2018). Figure 16.

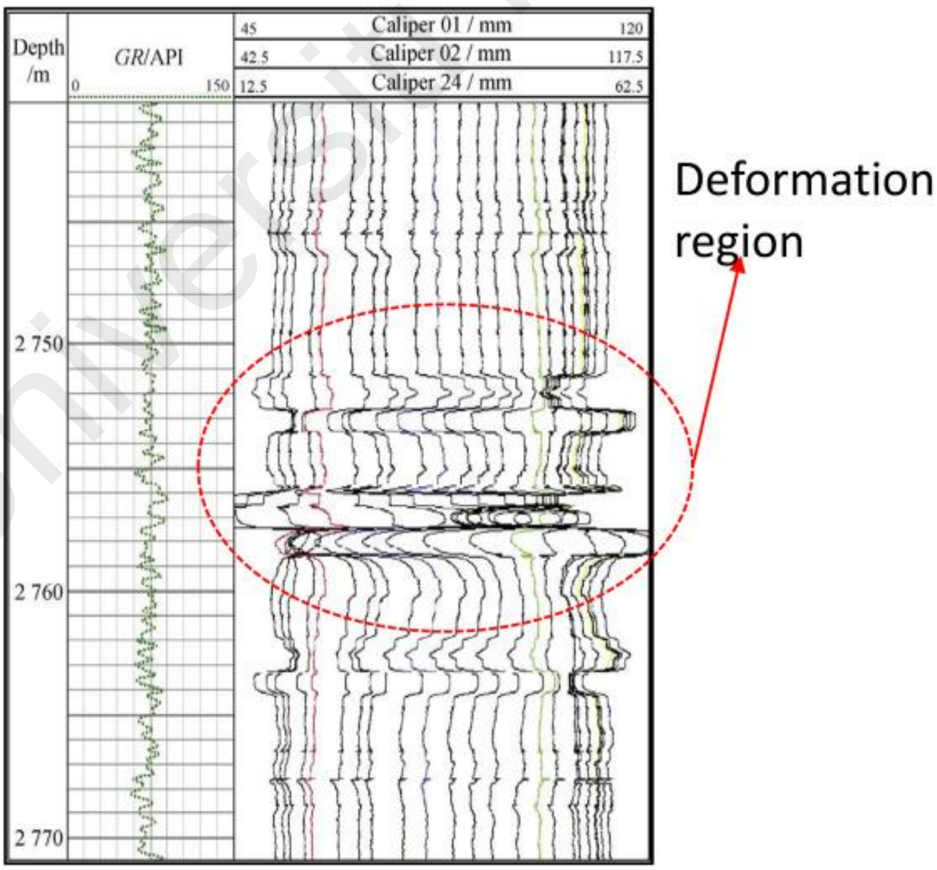

Figure 16: Typical well log signature showing casing deformation (Yin, Deng, et al., 2018; Yin & Gao, 2015; Yin, Han, et al., 2018).

2.6.2 Shear Failure

Shear failure of oil well casing occurs when formation of shear that happen to change in stress and pressure caused by the type of exploiting condition depletion, injection and heating. Shear failure is defined by Q. Wang et al. (2018) as a failure mechanism due to displacement of rocks strata along bedding plane or steeply inclined fault planes. During hydraulic fracturing process, fracture slips through the wellbore and induce shear load on the casing which as a result damages the casing under the action of formation shear slip as shown in Figure below.

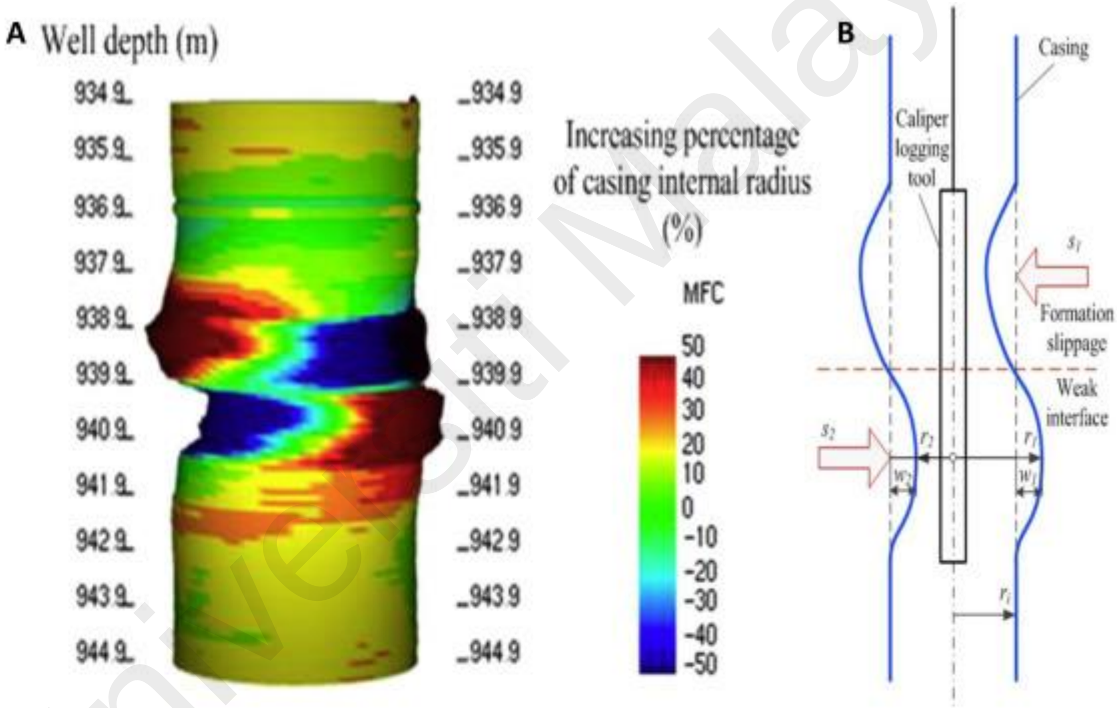

Figure 17: (A) Casing imaging logging of an injection well (B) Illustration of shear formation slip inducing casing failure (Yin, Deng, et al., 2018; Yin, Han, et al., 2018; Yin, Xiao, et al., 2018).

Furthermore, there is another reason for shear failure of casing which is water injection into the subsurface formation for pressure maintenance. Casing shear occurs at high differential pressure. Study shows that strain localisation is the primary reason of casing failure in Firebag oilfield. Conclusion showed that the lack of stress uniformity between the formation cement and the casing as one of the causes to this failure (Plaxton, Pehlke, Baxter, Crockett, & Kaiser, 2018). Figure 17.

2.6.3 Collapse or burst failure

It is established that the casing failures by collapsing or bursting is failure mode which is interconnected with one or more other failure modes; which is radial stress. Radial stress and failure mode of collapsing or bursting an oil well casing is understood that occurs due to tensile failure due to axial tension. As a result, the connection jump out due to severe compression or tension (Vudovich, Chin, & Morgan, 1988). During the production stages, the casing goes through multiple stresses, whereby the stresses change rapidly due to variable flow rates and dynamic loading. Kiran et al. (2017) recommended that the pressure void and cement channels at casing-cement interface could exert up to about 60% reduction on oil well casing collapse resistance. The failure is mainly attributed to unequal external load which exceed the casing yield strength, thereby causing the casing to collapse or burst. This collapsing failure is mainly classified into subcategories of yield, transitional, elastic, and plastic. On the other hand, researcher refutes this theory by pointing out that the primary reasons of the collapsing and bursting of the casing is due to factors influencing the casing's collapse resistance and arrived at a conclusion that the effects are small for 3D models with length to diameter (d/t) ratio above 10. Additionally, the increase in initial ovality would lead to a decrease in the pipe's resistance to collapse (Bastola, Wang, Mirzaee-Sisan, & Njuguna, 2014; Kuanhai et al., 2017).

Extensive studies and experiments were conducted in order to simulate the real-world conditions and induce burst stress in cemented wellbores using FEA under different operational conditions. It was concluded that, the cement has a much lower stresses which is approximately 40,000psi (von Mises Stress) which indicated of a decrease of 58.4%.

Therefore, this study showed that burst failure of casing is much likely un uncemented casing compared to a cemented especially in open hole completions (Fleckenstein, Eustes, & Miller, 2001). Therefore, in order to compensate this reduction in stress, allows the designers to design casings with a lower-yield pipe such as K55 (55,000 psi yield strength) or 379 MPa, or a lower weight casing with less wall thickness. In unconstrained case, pipe casing with a much higher yield strength is required; for example, N80 (80,000 psi yield strength) or 552 MPa.

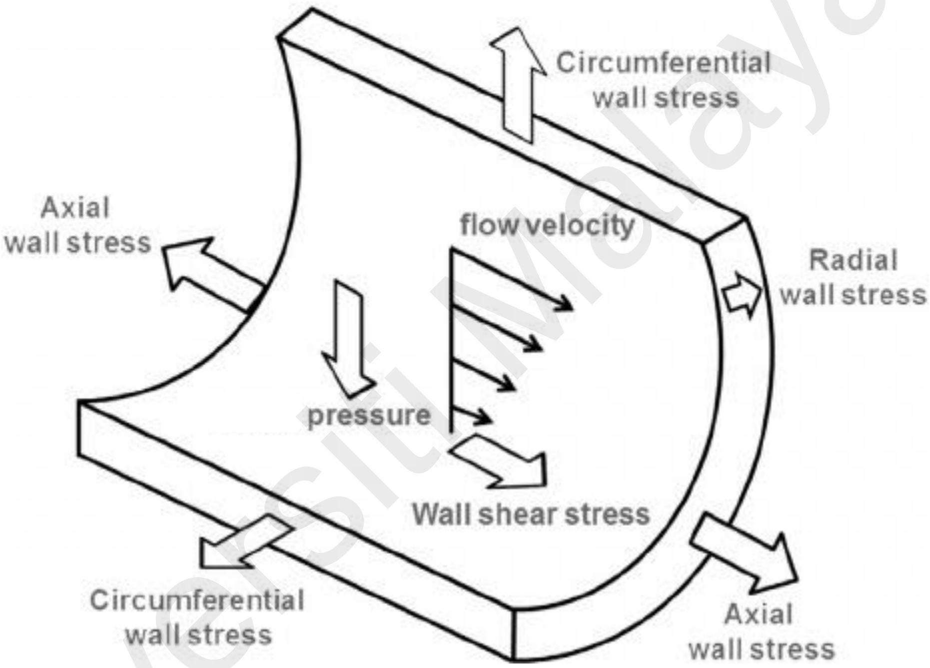

Figure 18: Pipe Stresses

During the thermal recovery in Canada where SAGD and CSS with typical operating temperatures of 199° C and increased casing yielding is a common phenomenon. Study showed that the body response when axial stress exceed the material yield strength do no address the API design equation for failure mode such as burst and collapse (Dall'Acqua, Hodder, & Kaiser, 2013). On the other hand, another study shows that casing burst stress in particulate annuli arrived at a conclusion that additional 5% of added support to cemented casing's nominal burst rating is provided by the casing grade bonded annulus fill material (Kalil & McSpadden, 2012). Figure 18, Figure 19.

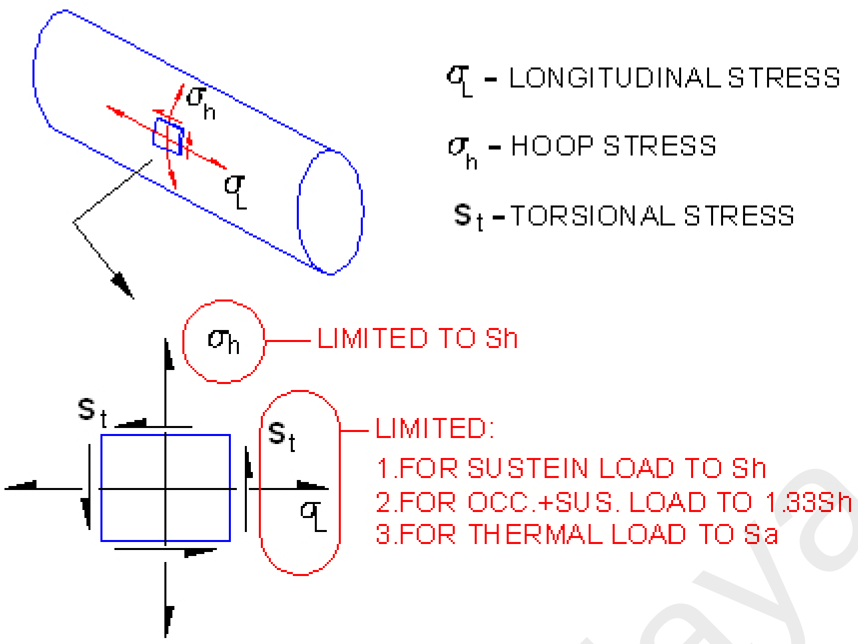

Figure 19: General pipe stresses illustration

2.6.4 Fatigue Failure

Fatigue stress in simple terms occurs when an object experiences nominal level of stress but in cyclic terms. This repeated localised and progressive cyclic load causes structural damage. Recent studies on the subject matter reported to have casing failures due to fatigue during multistage hydraulic fracturing especially at casing joints (Z. Liu, Samuel, Gonzales, & Kang, 2018). The study showed that cyclic stresses experienced by the casing during the fracturing processes with varying temperature between stages puts a toll on the casing itself. Fatigue load is experience mainly during the series of plugs and perforation and followed by fracturing process subject the casing into multiple loads triggering fatigue stress on the material. Production casing on the other hand experiences cyclic loading of both pressure and temperature during the fracturing process, whereby the net result constitutes to casing fatigue failure (Z. Liu et al., 2018).

The casing also goes through thermal axial compression and axial tensile stress during the steam injection process. The resulting alternation in tension and compression in cyclic terms also causes fatigue on the casing's structure (Y. Wu, Guo, & Zhang, 2017). Lim, Tellier, and Howells (2012) also indicated that casing in harsh conditions such as in stormy weather, waves, ocean currents, and other heavy motion at the sea causes the motion to be transferred down to the riser to the wellhead, conductor and casing system which can induce fatigue stress especially at the casing connectors (joints) as shown in Figure below. To add to this, in some studies indicated that cyclic thermal changes such as in geothermal wells, where the temperature gradient is more than other wells causes fluctuations in temperature and internal pressure. These fluctuations can subject the casing to variable loads capable of inducing fatigue failures. Thermal loads also have the potential to alter hoop and increase mechanical stresses considerable during injection process (Teodoriu, Ulmanu, & Badicioiu, 2008).

Study conducted to examine the failure causes of a 9 5/8" diameter K55 seamless casing during drilling of an oil well. As a result, fatigue crack nucleation and growth in the tube/coupling (T/C) transition zone was identified in the Fractographic analysis. Multiple fatigue cracks we identified in other casings which however did not lead to fracture. However, the stress analysis showed the physical and chemical material test and numerical stress analyses at the T/C threaded joints were subjected to loads during the drilling process. Hence, as a result, causing leaking during the well completion stage (Cirimello, Otegui, Carfi, & Morris, 2017). Researchers arrived at a conclusion future integrity of casing used for drilling could not be assured. Figure 20.

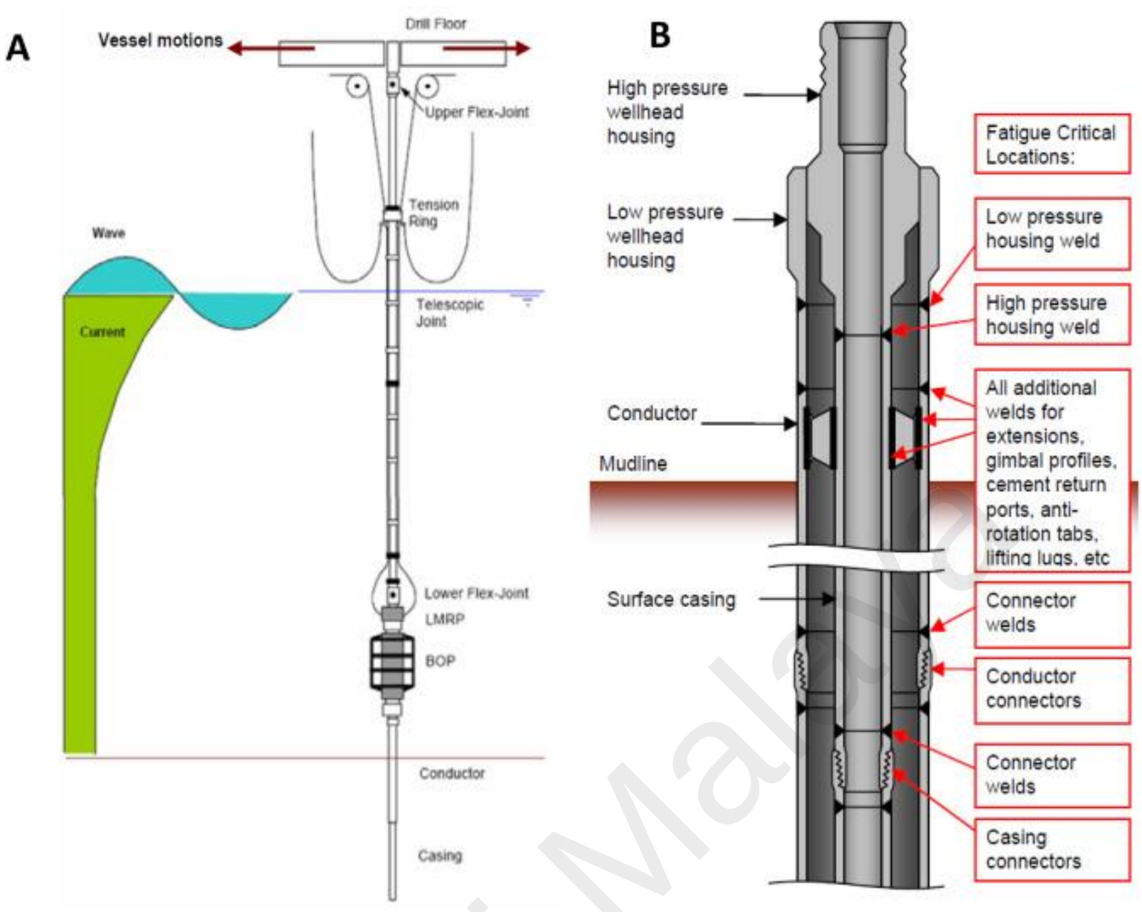

Figure 20: (A) Riser pipe stack-up and sources of motion (B) Fatigue critical locations (Lim et al., 2012).

2.6.5 Wear/erosion/corrosion failure

Wearing of casing is mostly occur due to frictional contact of the drill string with casing thereby exerting forces and gradually removing part of the surface of the casing. Gradually this surface friction induces forces and damages the structural integrity of the casing and eventually perforating or breaking the casing entirely. The thickness reduction is directly related to the force magnitude, contact area, angle, fluids and material strength (Mao, Cai, & Wang, 2018). Another research shows that corrosion develops when casing is exposed to corrosive environments resulting in cavities or perforation in extreme cases at both the inner and outer walls of the casing. Eventually this phenomenon leads to bursting and collapsing when under load, whereby the corroded casing will cause stress concentration, and degrade the casing strength entirely. Casing leak on average is expected whenever an average metal-loss value is between 30 and 70%, whereby the casing failure can be concluded when the metal loss is above 70% and no casing failure can be deduced if metal loss is below 30% (Lin et al., 2016; Yuan, Schubert, Teodoriu, & Gardoni, 2012). Furthermore, casing wear during directional drilling well also contributes to erosion of the well casing. This process causes casing strength degradation, casing deformation and even well abandonment. Studies showed that, with a combination of abrasive wear, erosive wear, and corrosive wear causes a nonlinear behaviour with increasing rotational speed of the drilling pipe, however this theory is not applicable in linear manner. Activity of the Cl-ions in the drilling fluids can also influence the formation and properties of the protective film on the casing surface, exponentially increasing the wear rate which is further attest to the nonlinear behaviour (Mao et al., 2018; Q. Zhang et al., 2016). Figure 21,Figure 22.

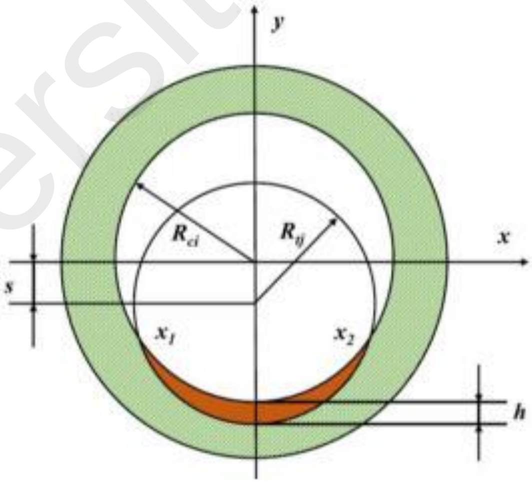

Figure 21: Schematic of casing wear (G. Zhang et al., 2011; Q. Zhang et al., 2016).

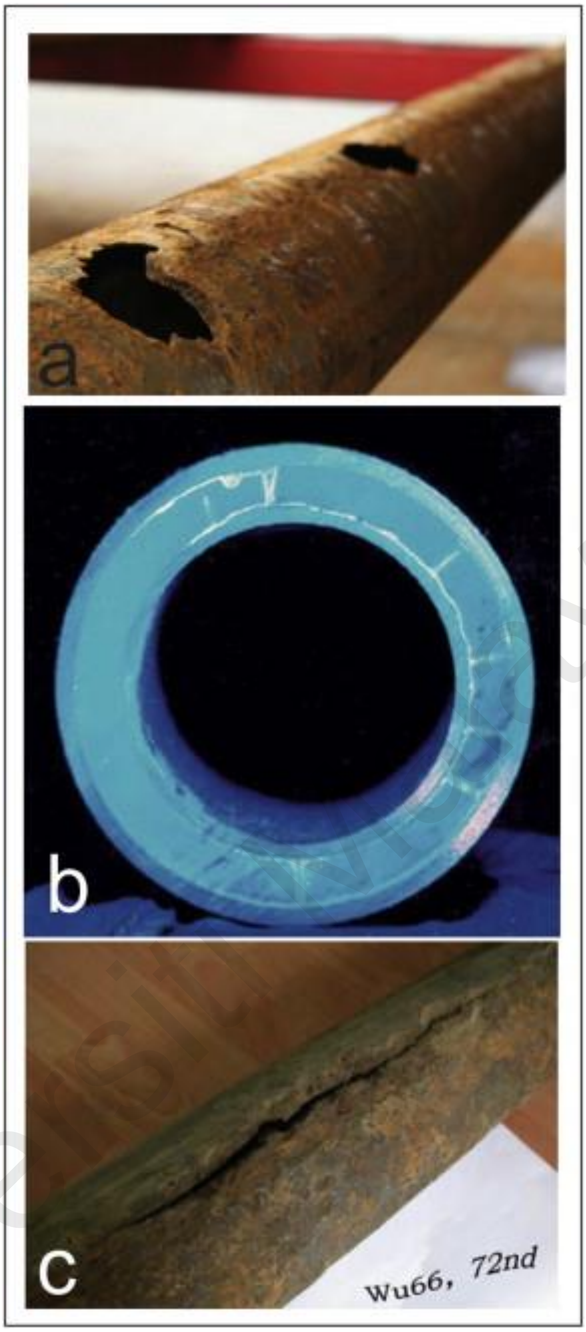

Figure 22: (a) Corrosion of tubing (Torbergsen et al., 2012).; (b) Crack in cement (CROOK, KULAKOFSKY, & GRIFFITL, 2003).; (c) Corrosion of casing (Xu, Yang, Li, & Chen, 2006).

2.6.6 Connection failure

During the process of cementing in horizontal wells, which is included with rotation of the casing in the lateral section is a common practice in the oil and gas industry. This is because rotation of the casing reduces/eliminate voids present in the cement slurry.

However, these rotations exert abnormal amount of force on the casing especially on the joints. High-rotating-bending loads exerted on the joints causes the failures of the casing. Horizontal wells connection do suffer such high and significant cycling loads causing the joint failure a more common occurrence (Hamilton & Pattillo, 2019). Other failures could also manifest either inclusive of casing connections and/or auxiliary equipment such as wellhead during the oil and gas production. Researchers have examined the relationship between structural casing and formation effects on wellhead motion due to temperature loads which eventually results in casing deformation. Studies concluded that semi-analytical model that can be applicable to study the various wellhead loading situations that can cause multiple failures and motion in the upward direction. Most common of the failures identified other than connection failure were local buckling, shear failure as the main types of failure on casing strings (Aasen & Pollard, 2003; Sathuvalli & Suryanarayana, 2016). Figure 23.

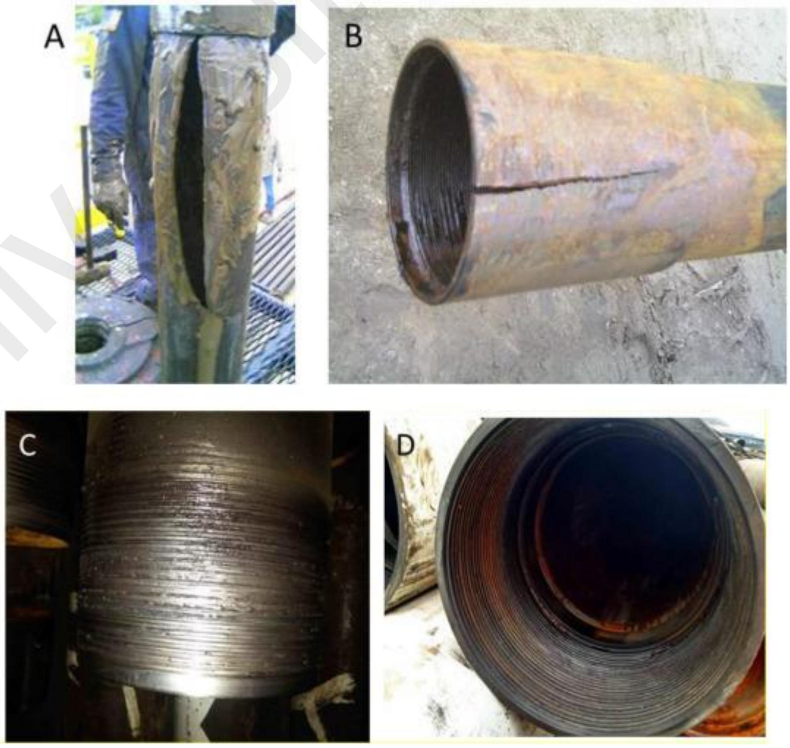

Figure 23: (A&B) typical example of connection failure. (C&D) presents pin and box thread damage. (Dusseault et al., 2001).

Both API and ISO have issued recommended practice for connection evaluation procedure (API RP 5CS and ISO/PAS 12835) for the much desired hydraulic fractured wells (Hamilton & Pattillo, 2019). During this modern era, where oil and gas production is pushed to new limits, the development of well projects pushes the connection and tubular performance to abnormal limits and inducing more failures. Operators around the worlds realised certain limitations to casing joints to reflect the well design requirement and load conditions of modern wells. This is crucial especially for offshore HPHT wells, where the consequences of connection failure can be catastrophic and extremely expensive.

2.6.7 Casing – cement-formation failure

Various well integrity issues can manifest with the casing and cement formation as discussed in the previous subchapters. However, research studies shows that we can magnify the most severe reasons of steel casing and cement sheath to two primary reasons. Those are induced stresses and downhole stress changes due to hydraulic fracturing, steam injection, well test during well operations. These failures can also be accelerated by chemical reactions as a result from corrosive substance present in the well. On the other hand, failure or damage suffer by the cement casing could also result in endangering the health state of casing and its connections. The integrity of casing-cement system is mutually inclusive; whereby the failure of casing undermine the cement integrity (W. Liu et al., 2017). In a study when simulated the effect of injecting surface fluids (sea water. CO_2 steam) in oil and gas reservoir, the final result indicated that the rock formation has an excessive impact on the stress of the casing (Ferla, Lavrov, & Fjær, 2009). The modelling of casing-cement and the formation system further revealed that in steam injection wells, the expansion and stress lead to cement failure behind the casing by cracking under high hoop stress. To make matters worse, cement, casing and formations system caused casing to fail in form of excessive deformation, buckling and collapse due to thermal expansion of the casing. Figuratively, as the parameters of injection exceeds 4.8MPa and 260° C (700psi and 500° F), the production casing fails (J. Wu & Knauss, 2006). As the temperature changes, the casing tends to expand/contract radially and tangentially which the causes the casing restrictions in axial directions causing more internal stresses to build up. However, in steam injection well, cement and formation are heated and all expand/contract based on their coefficients of thermal expansions. As a result, this result in different radial stress development at the casing-cement interface (Fang, Wang, & Gao, 2015; J. Wu & Knauss, 2006).

2.7 Summary

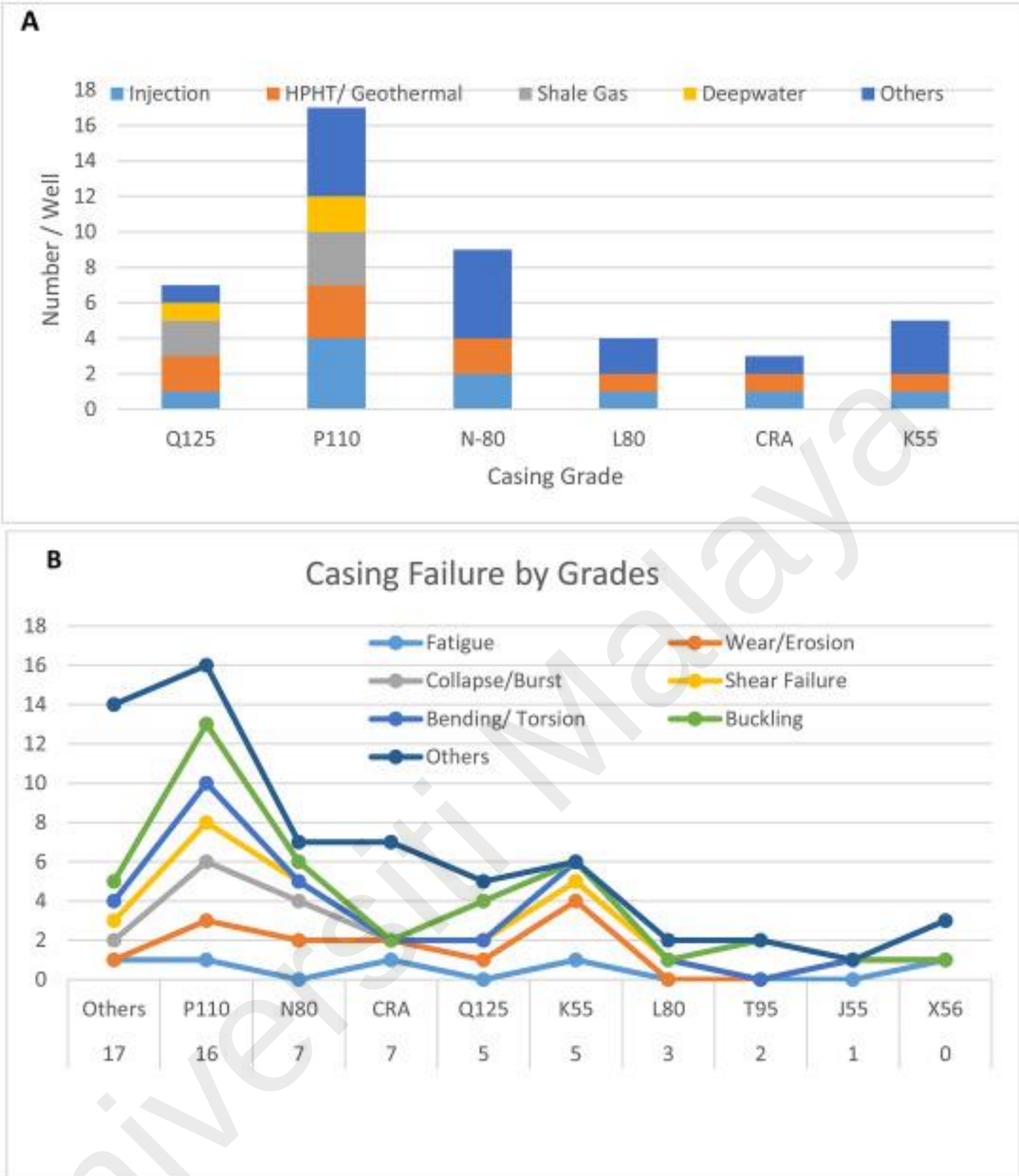

Figure 24: (A) Presents a concise summary of casing utilization by well type (B) Casing failure mix by grades on the articles reviewed. (Mohammed et al., 2019)

This section covered and investigated multiple failure scenario which are responsible of multiple types of casing failures. It is deducible that the casing failure occurs due to multiple types of casing experiencing failures due to various reasons. However, the reasons boil down to several main points which is responsible of all the failures. Those are, elevated temperature, and high load or stresses acting on the casing whether as a constant to cyclic behaviour pattern such as fatigue stress. These two primary conditions of the casing are the perfect condition for the creep deformation to occur on which very less research has been done. The major aim of the well construction is to produce oil and gas with no fluid leakage, barrier longevity and reliable well integrity throughout the well lifecycle. This chapter has included a comprehensive examination of literature which can support the theory and justification that conducted from previous research. It has further justified the theory proposed from previous study and provides a better insight regarding in next chapter, the research methodology will be reviewed and research design of the main requirements to casing that provides cementing of oil and gas wells during drilling and operation is their optimum centralisation, which allows achieving a better homogeneity of the slurry flow in the annulus. Optimum standoff between the borehole wall and the casing is ensured with special devices, centralisers put on the casing and spaced along it in a certain pattern. The paper offers a numerical solution to the centralisation of casing. The model includes 3D dynamic equations of the lateral and axial motion of a long pipe in the wellbore with constrained deflections in borehole during tripping operation considering all the major factors typical for casing exploration. A numerical method that enables to determine contact and friction forces as well as standoff between the borehole wall and the casing is proposed. Examples of standoff ratio calculations for casings of varying sizes and wells with different inclination and tortuosity are presented (D. Hayhurst & Webster, 1986a).

Table 4: Summary of widely used casing buckling and related buckling model

Buckling Model	Assumptions	Operation
Euler	Beyond critical load casing deflect/buckled in vertical wells	Injection of water leads to slippage of weak structural interfaces which cause buckling of casing
Lubunski	Buckling occur when effective axial force is applied	Volume fracturing led to casing axial deflection

Dawson & Paslay	Beyond critical load casing deflect/buckled in deviated wells	Volume fracturing activate faults and fractures which because several deform section in horizontal wells
Mitchell	Sinusoidal buckling occurs when critical force is less than effective axial force and effective force less than $2.8F_{cr}$. Helical buckling occurs before reaching $2.8F_{cr}$.	Horizontal well stimulation led to complex stresses on the casing which led sinusoidal buckling of casing

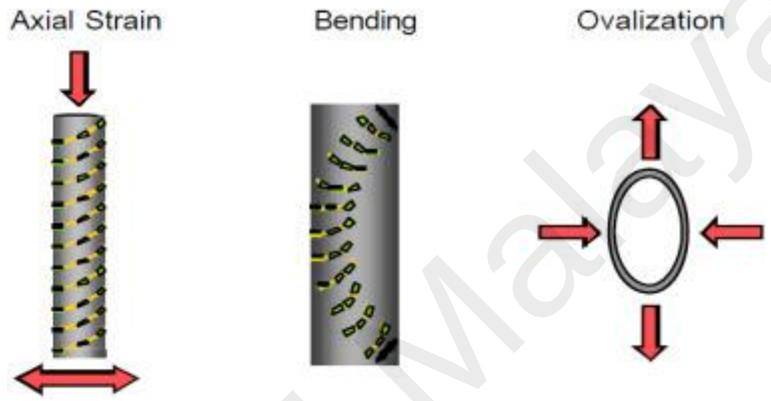

Figure 25: Models of well tubular deformation (Pearce et al., 2009).

CHAPTER 3: METHODOLOGY

3.1 Material characterisation

This section of the paper is intended to study the thermal and physical properties of the API 5CT J55 casing as well as the creep damage evolution. Thermal and mechanical properties of the casing as shown the table in the Appendix below, such as chemical composition, tensile strength, yields strength, dimension etc.

On the other hand, the most famous equation to study and predict the secondary creep is often done by Norton's power law equation:

Equation 1: Norton Power Law equation

$$\dot{\varepsilon}_{cr} = C_1 \sigma^{C_2} e^{-C_3/T} , \qquad (1)$$

Where $\dot{\varepsilon}_{cr}$ is the steady state creep strain rate, σ is stress (MPa), T is temperature (K), C_1, C_2, and C_3 are material constant which should be determined based on creep data.

Damage which is caused by creep can also be analysed by the damage evolution relationship which is given by the modified Lemaitre-Chaboche model (Xiangxin, Xueren, & Xiaojun, 2003):

Equation 2: Lemaitre-Chaboche equation

$$\frac{dD_C}{dt} = \left(\frac{\sigma}{A}\right)^r (1 - D_C)^{-k} , \qquad (2)$$

Where D_C is the creep damage, t is time (h), σ is stress (MPa), and k is given by:

Equation 3: L Lemaitre-Chaboche equation

$$k = a_o + a_1(\sigma - z) + a_2(\sigma - z)^2 , \qquad (3)$$

Where r, A, a_o, a_1, a_2, and z are the material constant which should be determined based on creep test data.

3.2 Simulation and Elongation Calculation Methods

String stress is mainly formed by interrelation between thermal field and stress field, so coupling of heat and structure in ANSYS is often applied in concrete analysis. Basic coupling method of heat and structure begins with thermal analysis and continues by loading the analysis results into structure stress analysis directly.

I. Fill in string structure parameter list, build finite element solid model, and choose thermal analysis;

Table 5: Structure Parameters for FEA

Casing	**Internal Diameter (mm)**	**Outer Diameter (mm)**	**Depth/m**
Ø88.9 mm (3 1/2") Insulated tubing	75.997	114.3	—
ø244.475 mm (9 5/8") Technical casing	232.49	244.48	1768
Ø339.72 mm (13 3/8") Surface casing	327.54	339.72	360
Ø508 mm (20") Riser pipe	495.3	508	96.2

II. Define property of different materials and apply to each solid.

III. Conduct mesh generation by using map mesh or sweep mesh.

IV. Conduct Glue operation on contact surfaces.

V. Define temperature boundary conditions and analyse temperature distribution.

VI. Carry on unit transformation of heat-structure.

VII. Define restrict conditions, import temperature analysis results, and load fluid and strata stress.

VIII. Conduct coupling analysis of thermal and structure and analyse the calculation results.

3.3 Simulation and elongation calculation method for API 5CT J55 casing

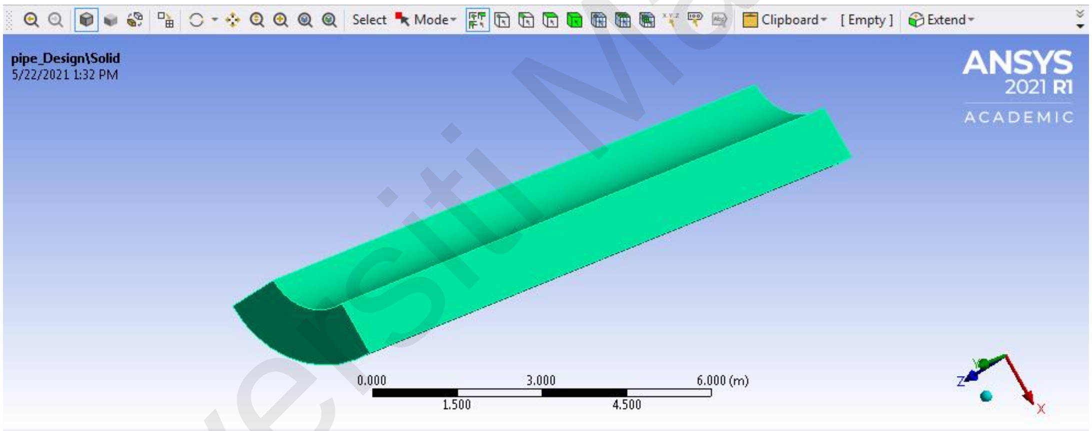

Figure 26: Geometry of the casing

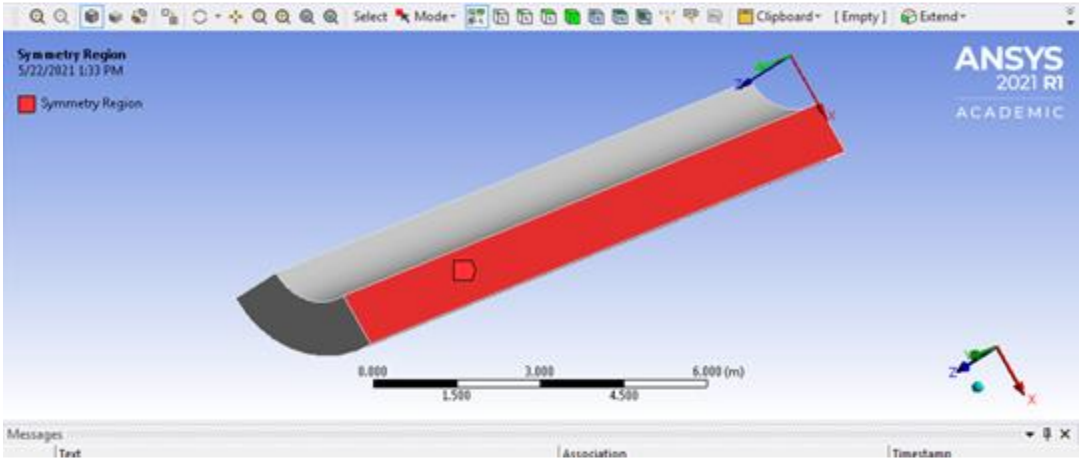

Figure 27: Symmetry region of the geometry design of casing structure

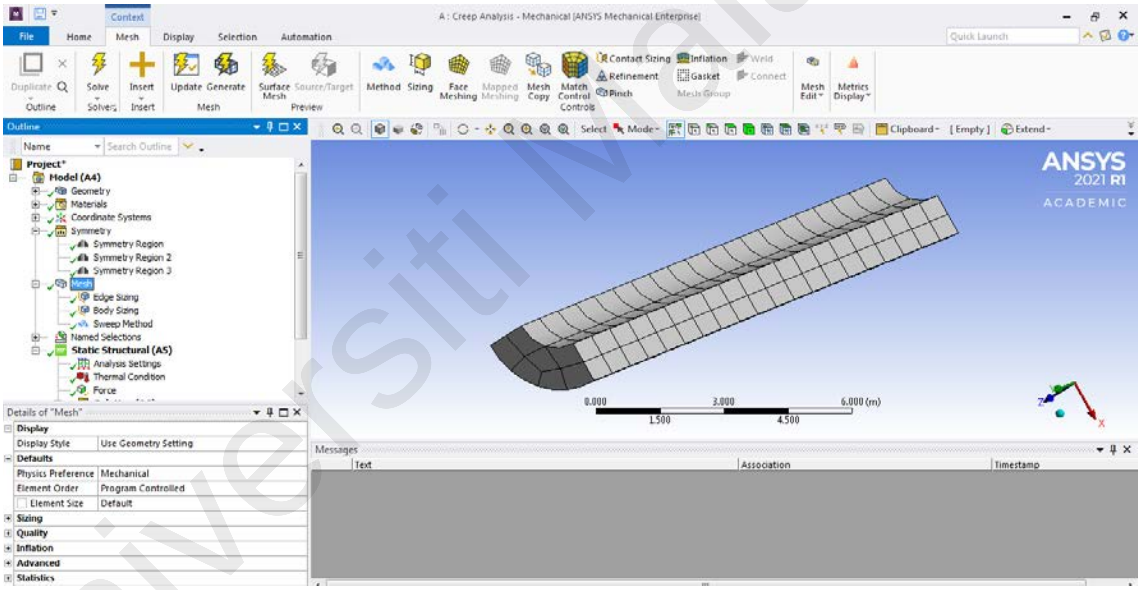

Figure 28: Meshing

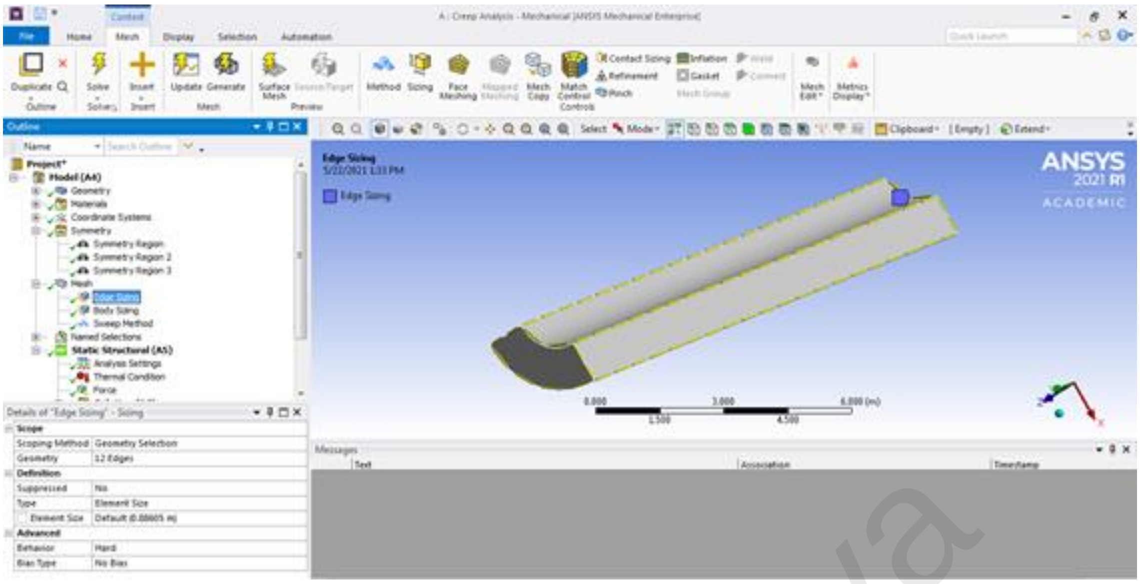

Figure 29: Edge sizing (ANSYS)

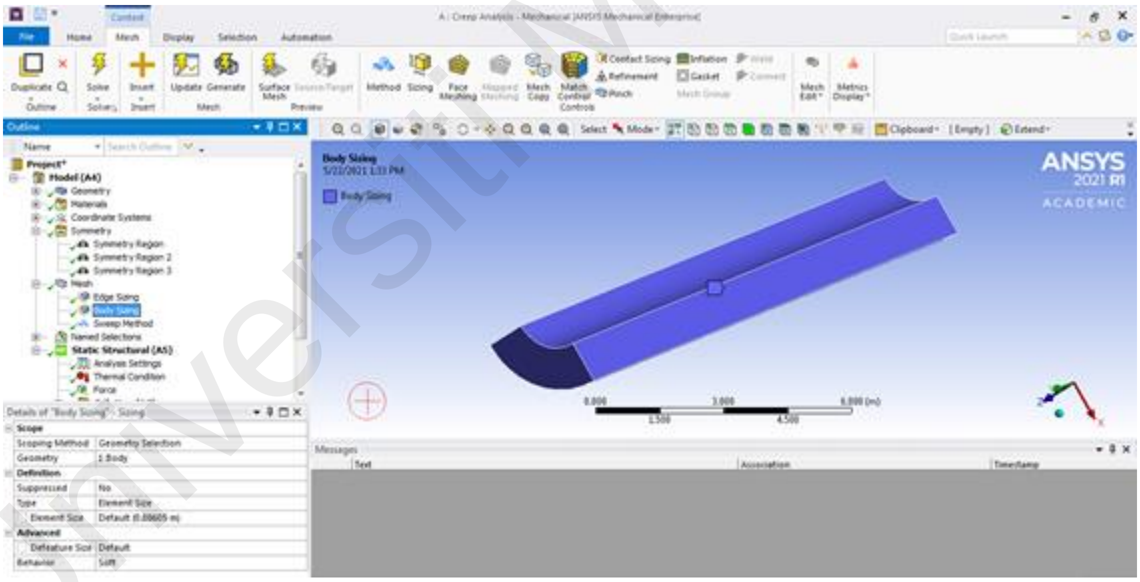

Figure 30: Body sizing (ANSYS)

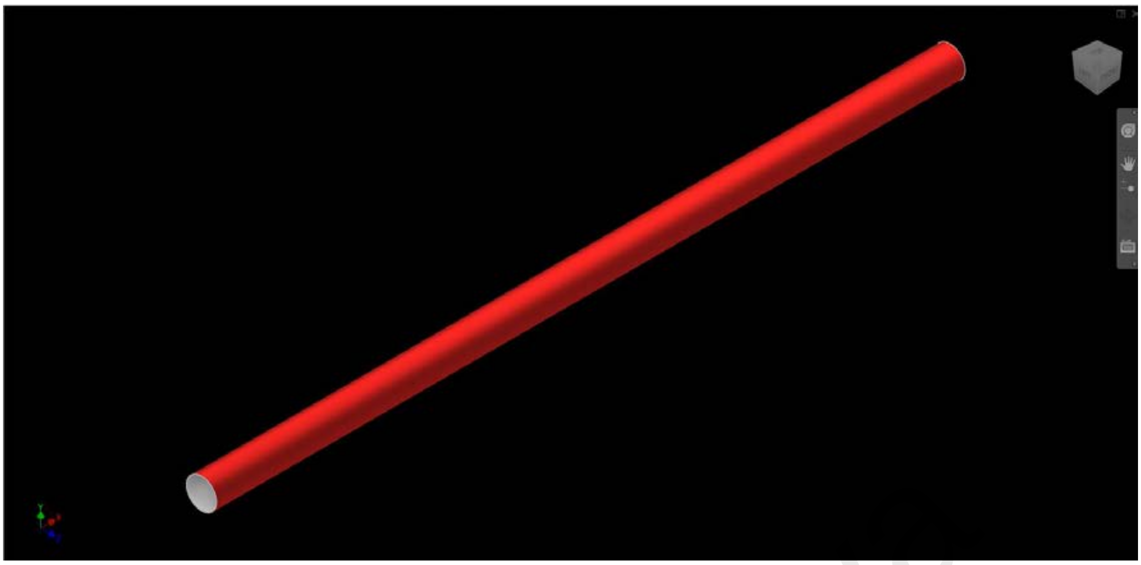

Figure 31: CAD Model of the casing

3.4 Simulations Conditions

ANSYS software (static structural) was used for the analysis of the simulation sample in order to simulate the real-life conditions and its effect on the oil well casing.

3.4.1 Geometry (Simulations Sample Dimensions)

Details of "Geometry"

Definition	
Source	C:\Users\SarmadKhubaibSarajun\OneDrive - Asia ...
Type	DesignModeler
Length Unit	Meters
Element Control	Program Controlled
Display Style	Body Color
Bounding Box	
Length X	2. m
Length Y	17.55 m
Length Z	2. m
Properties	
Volume	41.352 m^3
Mass	3.2461e+005 kg
Scale Factor Va...	1.
Statistics	
Bodies	1
Active Bodies	1
Nodes	932
Elements	140
Mesh Metric	None
Update Options	
Basic Geometry Options	

Figure 32: Geometry Dimensions

The length of the material is used with a dimension of *17.55m* and *2m* wide with a symmetrical sided on both faces. The total volume of the simulation sample is $41.352m^3$. A section of the sample is considered for the simulation is to represent the entire structure with a symmetrical sample to consider how does it behaves under the simulation. Figure 31.

3.4.2 Material Properties

Details of "Structural Steel"

Common Material Properties	
Density	7850 kg/m³
Young's Modulus	2e+11 Pa
Thermal Conductivity	60.5 W/m·°C
Specific Heat	434 J/kg·°C
Tensile Yield Strength	2.5e+08 Pa
Tensile Ultimate Strength	4.6e+08 Pa
Nonlinear Behavior	False
Full Details	Click To View Full Details
Statistics	
Assigned Bodies	1

Figure 33: Mechanical Properties of the material

Engineering Data: Material View

Structural Steel

Fatigue Data at zero mean stress comes from 1998 ASME BPV Code, Section 8, Div 2, Table 5-110.1

Density	7850	kg/m³
Structural		
Isotropic Elasticity		
Derive from	Young's Modulus and Poisson's Ratio	
Young's Modulus	2e+11	Pa
Poisson's Ratio	0.3	
Bulk Modulus	1.6667e+11	Pa
Shear Modulus	7.6923e+10	Pa
Isotropic Secant Coefficient of Thermal Expansion	1.2e-05	1/°C
Compressive Ultimate Strength	0	Pa
Compressive Yield Strength	2.5e+08	Pa
Strain-Life Parameters	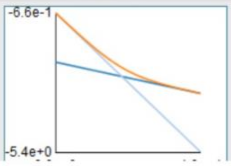	

Figure 34: Mechanical Properties of the material (2)

The material properties considered is structural steel with a young's modulus of 2×10^{11} Pa and Poisson's Ratio of 0.3 for the simulation. Figure 33, Figure 34.

3.4.3 Analysis Settings (Structural)

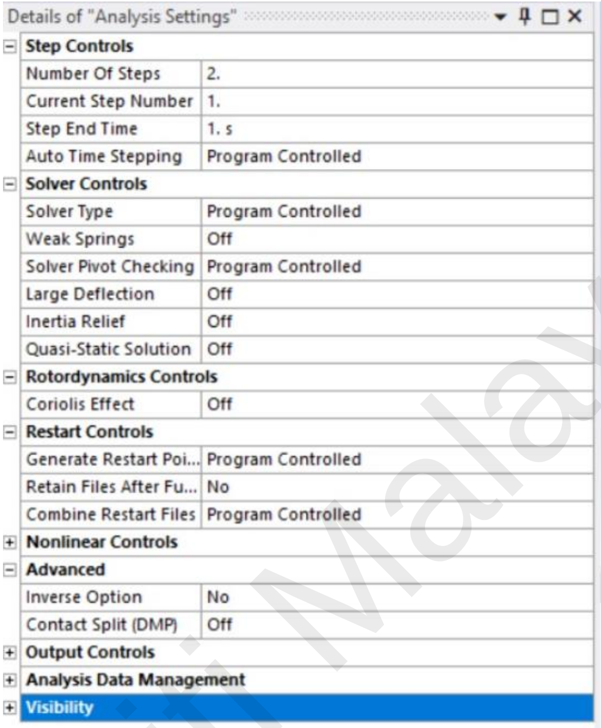

Details of "Analysis Settings"

Step Controls	
Number Of Steps	2.
Current Step Number	1.
Step End Time	1. s
Auto Time Stepping	Program Controlled
Solver Controls	
Solver Type	Program Controlled
Weak Springs	Off
Solver Pivot Checking	Program Controlled
Large Deflection	Off
Inertia Relief	Off
Quasi-Static Solution	Off
Rotordynamics Controls	
Coriolis Effect	Off
Restart Controls	
Generate Restart Poi...	Program Controlled
Retain Files After Fu...	No
Combine Restart Files	Program Controlled
Nonlinear Controls	
Advanced	
Inverse Option	No
Contact Split (DMP)	Off
Output Controls	
Analysis Data Management	
Visibility	

Figure 35: Analysis (Static Structural) ANSYS Settings

The analysis settings are set as shown in Figure 35 above.

3.4.4 Thermal Conditions

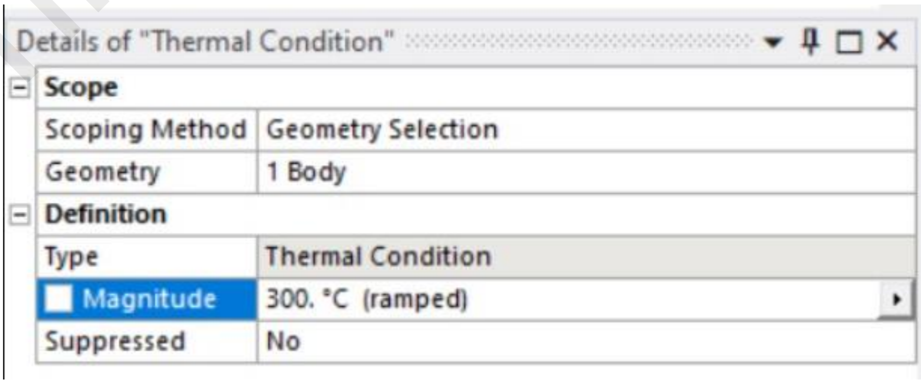

Details of "Thermal Condition"

Scope	
Scoping Method	Geometry Selection
Geometry	1 Body
Definition	
Type	Thermal Condition
Magnitude	300. °C (ramped)
Suppressed	No

Figure 36: Thermal conditions

As shown in Figure 36 above, the Thermal conditions of the Structure is set at 300°C which is at the higher end of the spectrum. As stated in Table 8, the temperature of the fluid fluctuates between 260°C and 270°C. Thus, of the simulation analysis purposes, a higher end temperature is considered to observe their adverse effect.

3.5 Summary

According to the investigation, concurring to the examination, the most necessities to casing that gives cementing of oil and gas wells amid penetrating and operation is their ideal centralisation, which permits accomplishing a stronger homogeneity of the slurry stream within the annulus. Ideal standoff between the borehole divider and the casing is guaranteed with extraordinary gadgets, centralisers put on the casing and dispersed along it in a certain design. This paper offers a numerical arrangement to the centralisation of casing. The demonstrate incorporates 3D energetic conditions of the horizontal and hub movement of a long pipe within the wellbore with obliged avoidances in borehole amid stumbling operation considering all the major components for casing investigation.

CHAPTER 4: RESULT AND DISCUSSION

4.1 Overall Conditions

As shown in Figure 37: Well Structure, wellbore structure parameter is shown in Table 9: , environment parameter is shown in Table 6: Environmental parameter, and thermal injection parameter is shown in Table 7: Thermal Injection Parameters respectively. These figures and tables show the environmental parameters and physical parameters of the wellbore structure and their behaviour. Referring to the details, dimensional parameters assumed, which are the riser's pipe is 96.2 m long in length with 39 m of length being in the air, 12 m in seawater, and 45 m in strata. The overall length of the surface casing is 360 m long. Considering the thermal coefficients of the air, seawater and strata are much indifferent compared to each other. Therefore, the relative impact of each condition on the pipe deformation are different to one another based on the temperature distribution of the casings. The simulation of the elongation is hence conducted in the air, seawater and strata for more accurate results of the oil well structure.

4.2 Temperature Distribution calculations

4.2.1 Wellbore's Heat Transfer under Seawater

The thermal resistance of the insulated tubing, annular convection of nitrogen injection, cement and strata heat resistance in radial direction, heat transfer resistance of radiation, as well as the impacts of the air, seawater and strata in axial direction. Therefore, the total temperature coefficient was obtained along the well bore as shown in Figure 38. On the other hand, heat loss distribution along the wellbore is shown in Figure 39. From the analysis of the results obtained from the figures, the primary heat loss distribution exerted is in the seawater, and comparatively lesser in the air and the most minimum in the strata.

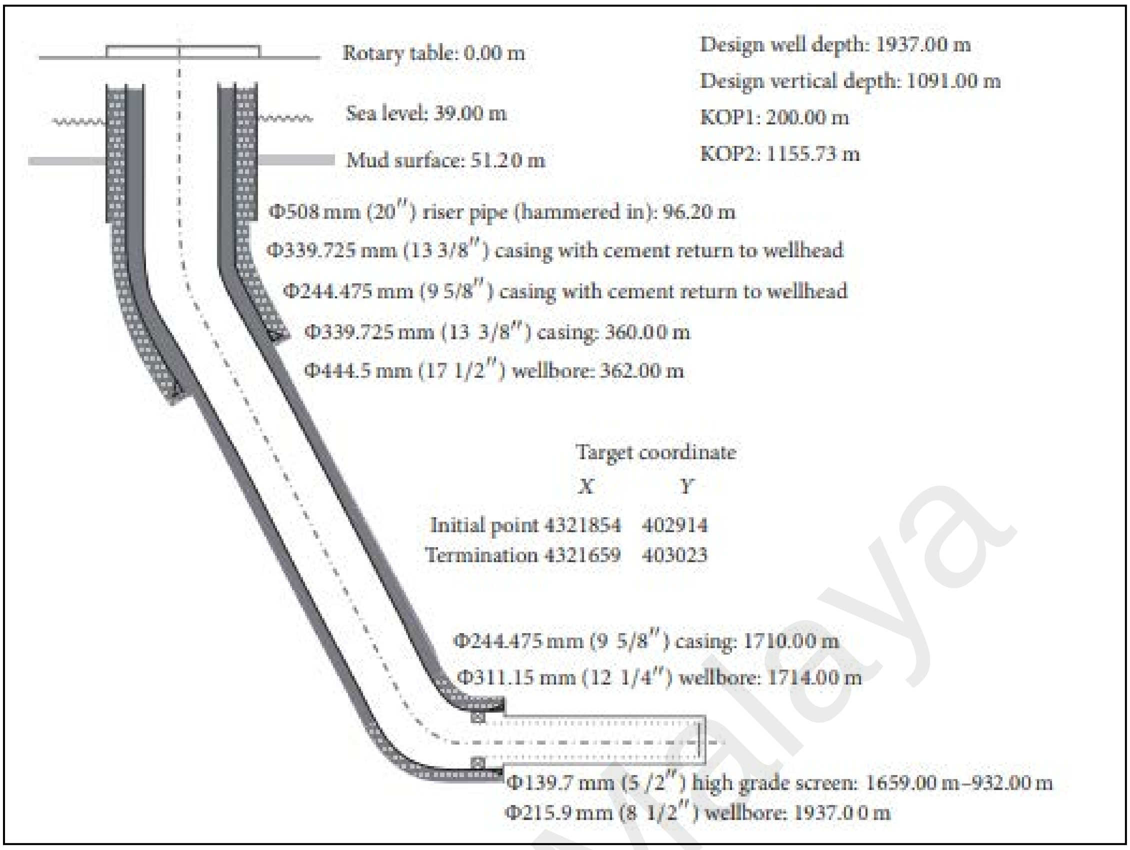

Figure 37: Well Structure

Table 6: Environmental parameter

String length in the air/m	39	**String length in seawater**	12.2
Thermal coefficient of insulated tubing/[W·(m^{-1}·K^{-1})]	0.02	**Thermal coefficient of cement/[W·(m^{-1}·K^{-1})]**	0.35
Thermal coefficient of strata/[W·(m^{-1}·K^{-1})]	1.743	**Temperature coefficient of strata/(m^{2}·s^{-1})**	10~6
Geothermal gratitude/(°C·m^{-1})	0.03	**Air temperature/°C**	20
Seawater temperature/°C	15	**Wind speed/(m·s^{-1})**	3
Seawater flow speed/(m·s^{-1})	0.5	—	—

Table 7: Thermal Injection Parameters

Expense of the air/(kg·h−1)	3000	**Injection temperature/∘ C**	270
Expense of diesel oil/(kg·h−1)	200	**injection pressure/MPa**	18
Injection rate of hot water/(kg·h−1)	8000	**Injection pressure of nitrogen/MPa**	18
Injection rate of all thermal fluid/(kg·h−1)	11200	**Injection rate of nitrogen/(Nm3 ·h−1)**	500

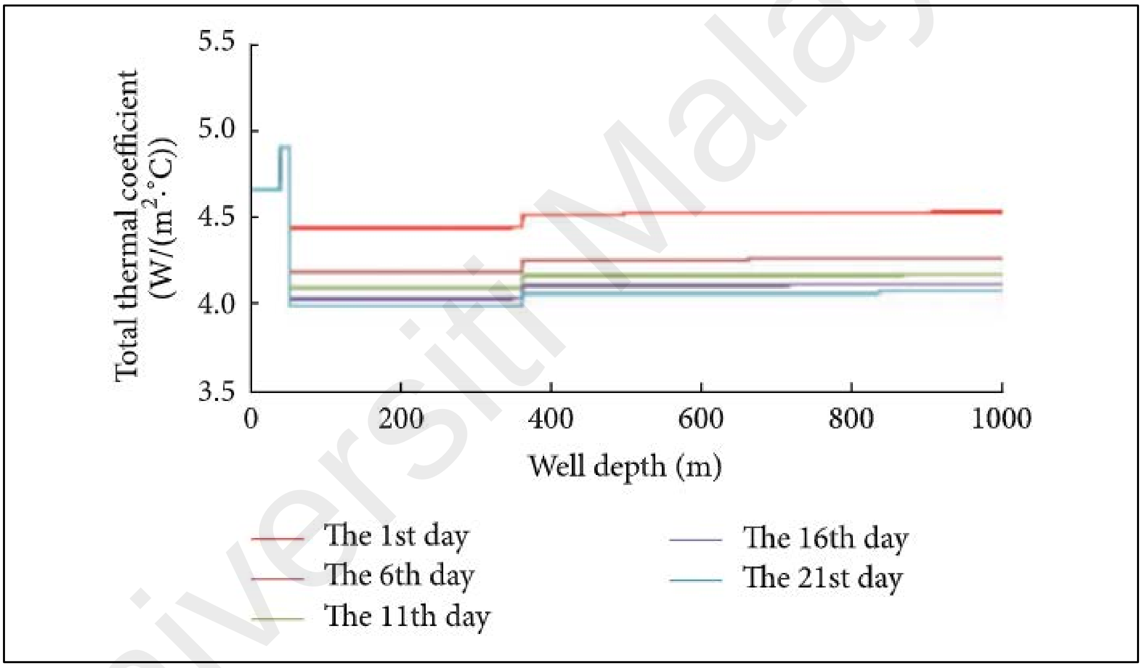

Figure 38: Thermal coefficient along wellnore.

Table 8: Temperature distribution to Completion

Depth/m	Fluid temperature/°C	ø244.475 mm (9 5/8″) casing temperature/°C	Cement boundary temperature/°C	ø399.725 mm (13 3/8″) casing temperature/°C	Cement sheath boundary temperature/°C	ø508 mm (20″) pipe temperature/°C
0	270	119.56	82.43	82.43	34.57	34.57
10	269.84	119.5	82.39	82.39	34.56	34.56
20	269.68	119.43	82.35	82.35	34.55	34.55
30	269.51	119.36	82.3	82.3	34.54	34.54
40	269.34	106.13	66.39	66.39	15.18	15.18
50	269.17	106.06	66.36	66.36	15.18	15.18
60	269.02	141.45	109.32	109.32	67.91	67.91
70	268.87	141.53	109.46	109.46	68.12	68.12
80	268.72	141.62	109.6	109.6	68.33	68.33
90	268.58	141.7	109.74	109.74	68.54	68.54
100	268.43	141.79	109.88	109.88		
190	267.12	142.54	111.14	111.14		
280	265.82	143.29	112.39	112.39		
360	264.66	143.96	113.51	113.51		

Table 9: Structure parameters of the wellbore

String	ID/mm	OD/mm	Depth/m
Ø88.9 mm (3 1/2″) Insulated tubing	75.997	114.3	—
ø244.475 mm (9 5/8″) Technical casing	232.49	244.48	1768
Ø339.73 mm (13 3/8″) Surface casing	327.54	339.73	360
Ø508 mm (20″) Riser pipe	495.3	508	96.2

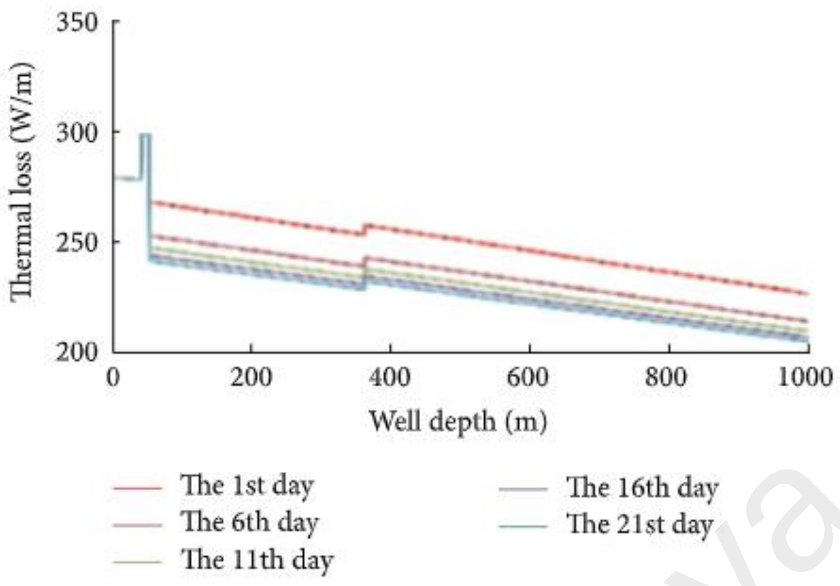

Figure 39: Thermal loss along wellbore

Heat transfer analysis as presented in Table 8 which includes the casing dimension including the ø244.475 mm (9 5/8") casings, the 1st cement sheath, the ø399.725 mm (13 3/8") casings, the 2nd cement sheath, and the ø508 mm (20") casings.

4.3 Creep Strain of the Material

As shown in the Figure 40 below, it is observable that the yield strength of the J55 steel reduces over time as the temperature increases, as well as the result for other materials behave the same. The curve of J55 shows that the strength of the material depleted not much until 200°C, however, after 200°C to 350°C the strength curve plunges at a higher rate to 0.7.

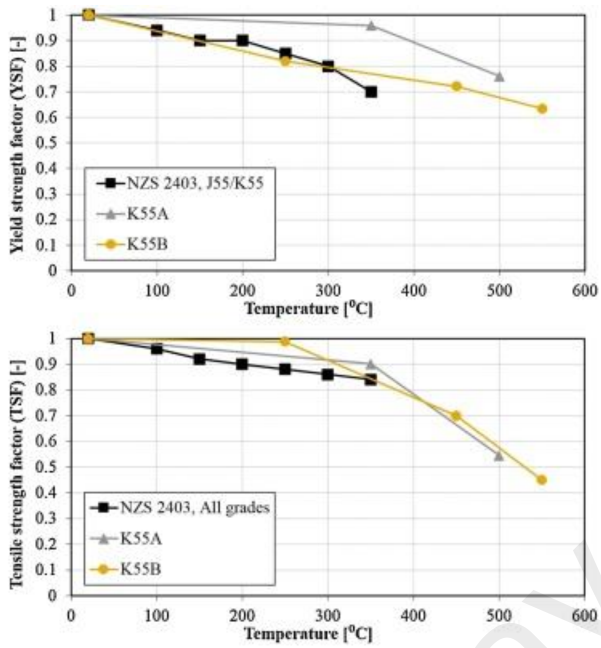

Figure 40: Creep Strain of the Material

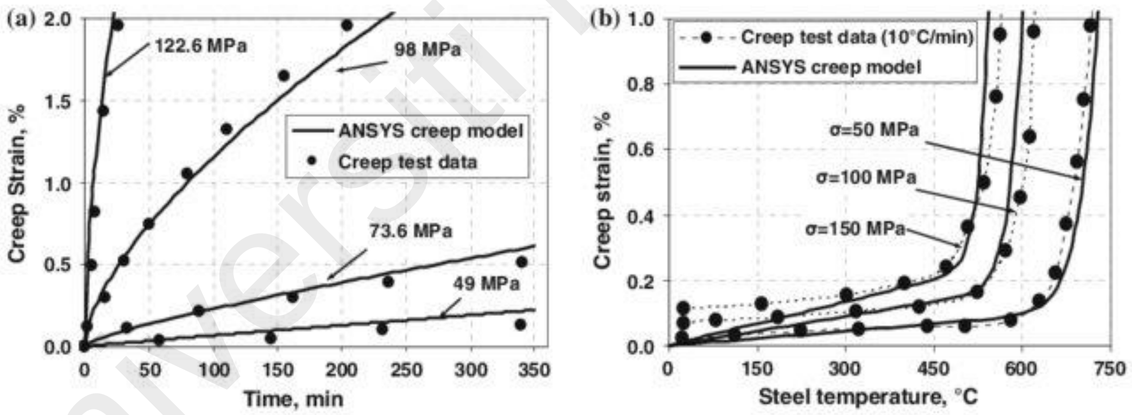

Figure 41: Creep Strain model

The creep model showed in Figure 41 above shows the curve of creep strain at three different stresses and temperature. It is deducable that as the stress increases, the creep strain exponentially increases and fractures at a lower temperature. Therefore, the higher the stress, or the higher the temperature, the higher the creep strain rate.

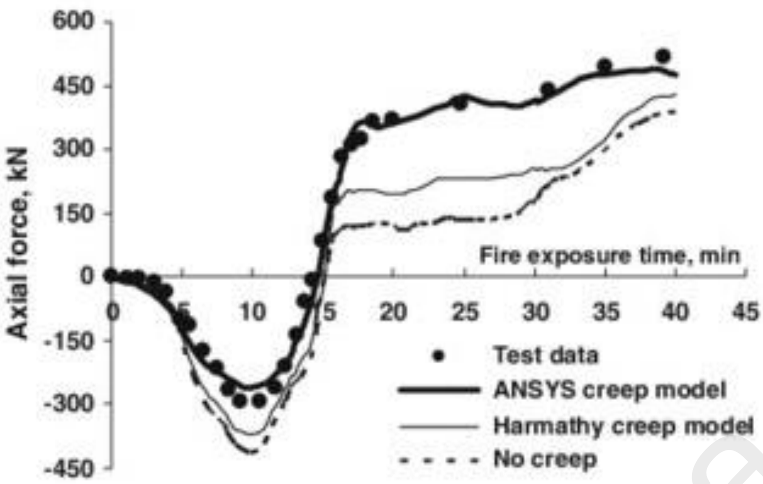

Figure 42: Creep Model

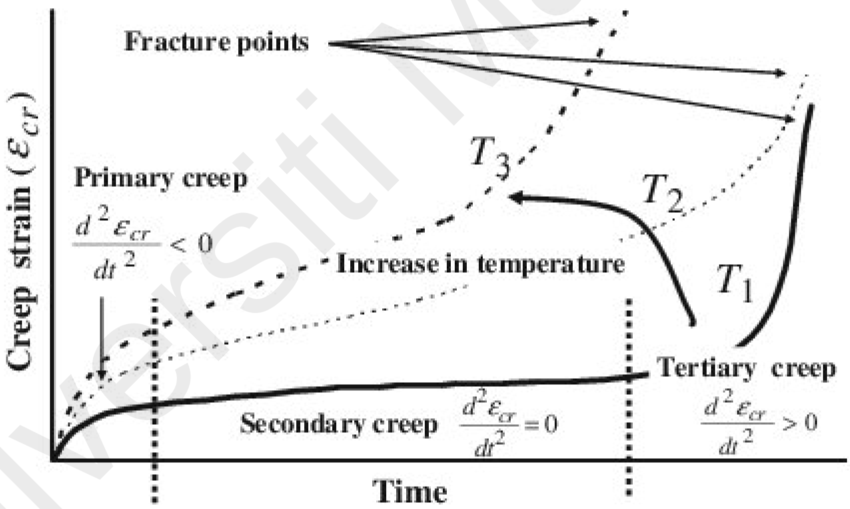

Figure 43: Creep Model curve

Figure 42 and Figure 43 above shows the creep model curve in which the laws of creep deformation. The ANSYS creep model indicates that when a material subjected to heat for a certain period of time, the creep deformation initiated in the microstructure of the metal and over time advances to secondary and tertiary creep stage.

4.4 ANSYS simulations

Table 10: ANSYS Simulation result summary

NO.	RESULTS	MINIMUM	MAXIMUM	AVERAGE
1	Total deformation	$2.501 \times 10^{-9}\ m$	$1.4645 \times 10^{-7}\ m$	$7.3507 \times 10^{-8}\ m$
2	Elastic Strain Intensity	$1.0827 \times 10^{-8}\ m/m$	$1.0866 \times 10^{-8}\ m/m$	$1.084 \times 10^{-8}\ m/m$
3	Stress Intensity	$1665.7\ Pa$	$1671.7\ Pa$	$1667.7\ Pa$
4	Volumetric Change	$0.26113\ m^3$	$0.33971\ m^3$	$0.30042\ m^3$

4.4.1 Total deformation of casing structure

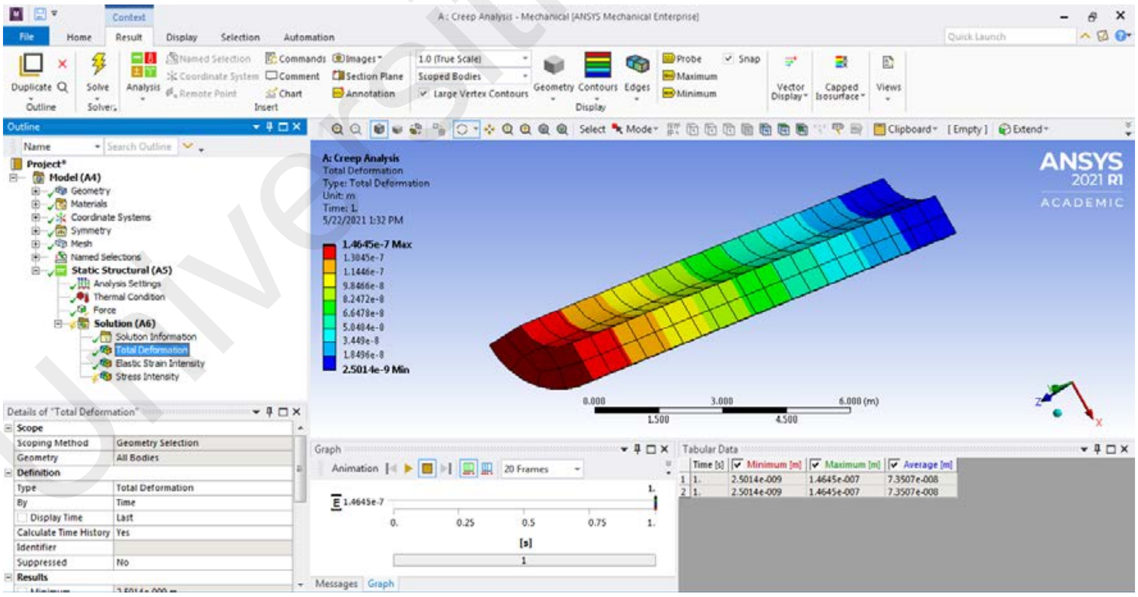

Figure 44: Total deformation (creep analysis)

Figure 44 above shows the deformation analysis of the casing's structure. The result of the analysis shows that the maximum deformation was $1.4645 \times 10^{-7}\ m$ with a minimum deformation of $2.501 \times 10^{-9}\ m$. This makes the average deformation of the casing structure of about $7.3507 \times 10^{-8}\ m$. The total deformation is acted on the edges and outer exterior of the casing. This makes the casing experience more hoop stress as well as radial stress during the oil well production. The casing joints are as well experience the most deformation concentration which makes it more susceptible to fail at the joints of the casings.

4.4.2 Elastic Strain Intensity

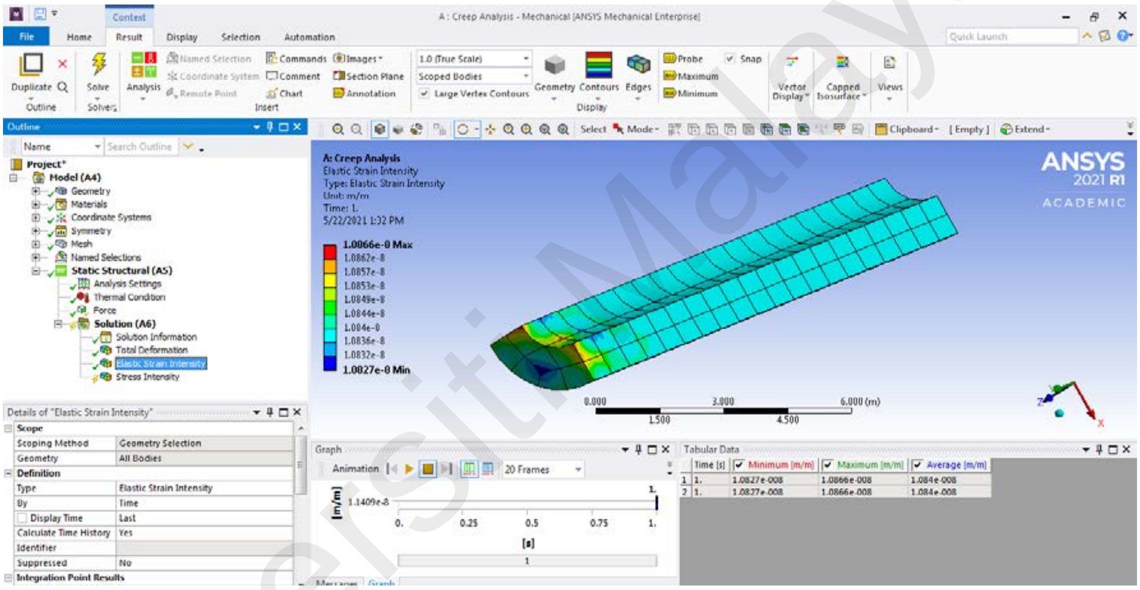

Figure 45: Elastic strain intensity (creep analysis)

Figure 45 above shows the simulation result of Elastic strain intensity occurred on the casing structure. The result from the ANSYS simulation is $1.0866 \times 10^{-8}\ m/m$ for the maximum, and $1.0827 \times 10^{-8}\ m/m$ for the minimum. The average elastic strain intensity of $1.084 \times 10^{-8}\ m/m$.

4.4.3 Stress Intensity

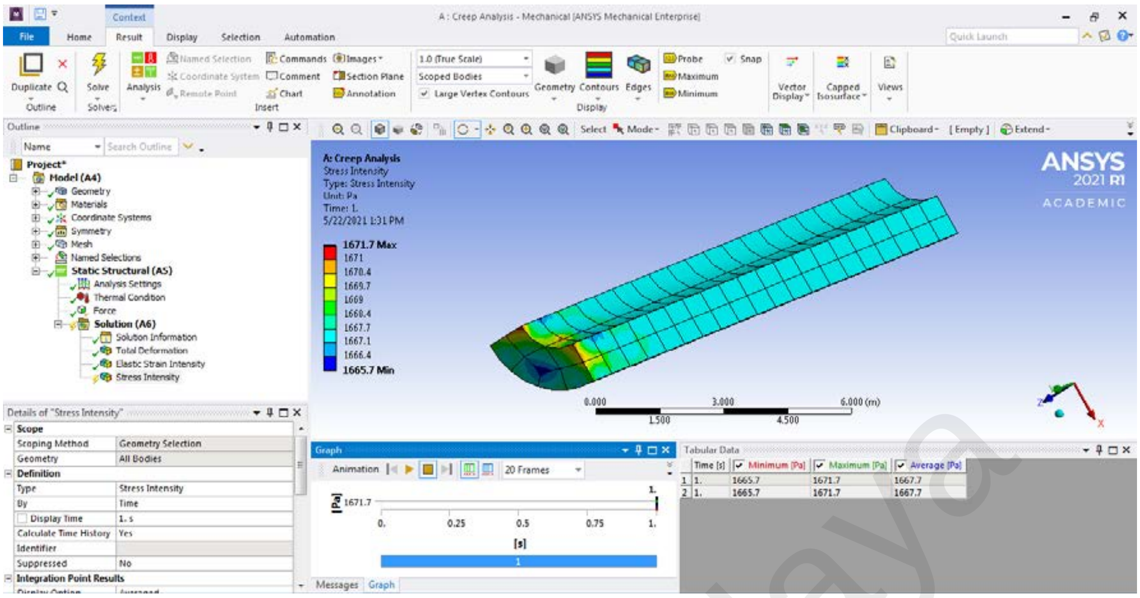

Figure 46: Stress Intensity (creep analysis)

Figure 46 and Table 10 above shows the simulation result of Stress Intensity experienced by the casing. The result from the ANSYS simulation of the average stress intensity is 1667.7 Pa.

4.4.4 Volume changes due to creep deformation

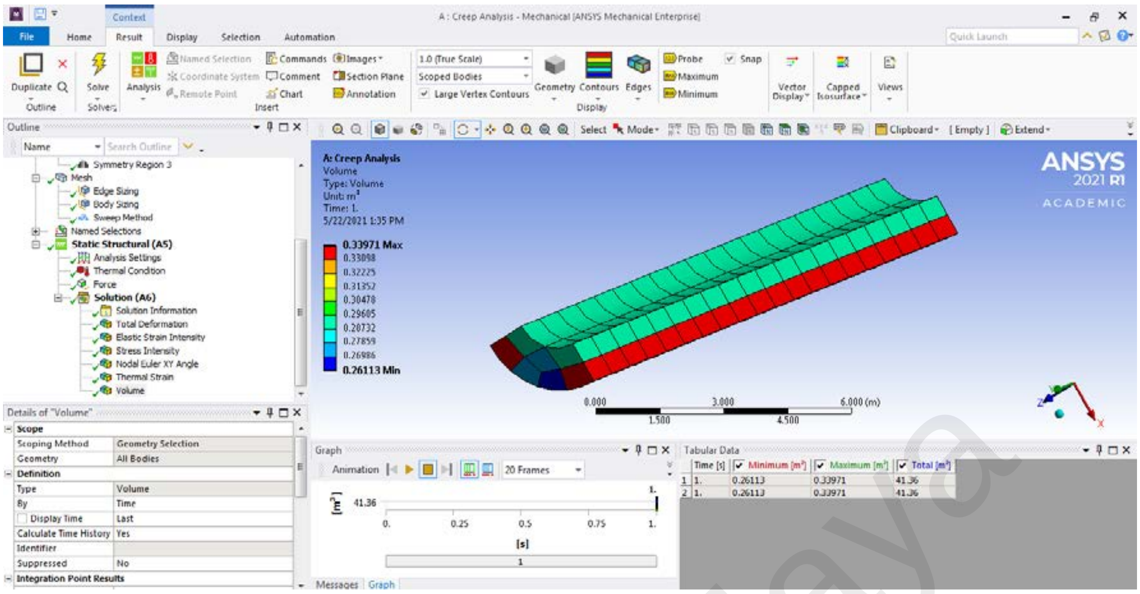

Figure 47: Volumetric changes due to creep deformation (creep analysis)

Figure 47 above shows the simulation result of volumetric change that occurred on the casing structure. The result from the ANSYS simulation is 0.26113 m^3 for the maximum, and 0.33971 $m^3$for the minimum. The average elastic strain intensity of 0.30042 m^3. These volumetric changes, as shown in the figure above, is experienced primarily on the outer parts of the casing. Therefore, the outer casing parts experiences tension within the substructure whereas the internal casing structure experiences compression.

4.5 Stress Distribution to All Casings

4.5.1 Meshing, operation to Simulate and Results

The casing is considered meshing which is to simulate bond state, cement, and casings. A model was built of the riser pipe-surface casing and production casing. The dimension of the which is mentioned in 4.1, which are diameter of ø244.475 mm (9 5/8”) for the production casing, and ø399.725 mm (13 3/8”) for the surface casing, and ø508 mm (20”) for the riser pipe. The contact surfaces were glued the contact surfaces in order to produce the meshing. Element brick 8 node of 70 which is a hexahedron element with 8 nodes was considered. In which these elements transfers heat in three dimensional with each node having only one temperature degrees of freedom (DOF). 3D heat analysis in both static and momentary was used and is able to generate a uniform heat current. Furthermore, a solid structure of element brick 8 node 45 was transferred from this element for relevant structure analysis. Figure 48.

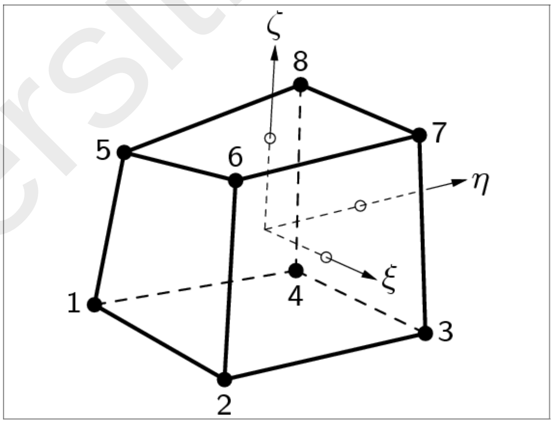

Figure 48: Brick 8 nodes model

The sweep mesh generation was conducted respectively for each part of the well bore for the analysis. Meshing results as shown in Figure 28 was generated with a symmetrical geometry shown in Figure 27. The temperature distribution results based on the analysis of complex thermal fluid was obtained as well as temperature boundary conditions for all casings was defined as per shown in Figure 39. Referring to the previous temperature distribution analysis, heat-structure coupled analysis was conducted. To facilitate the calculations the downhole string was divided into air and seawater section (0 ~ 51.2 m), the strata section 1 (51.2~96.2 m), strata section 2 (96.2~360 m), and strata section 3 (360~1710 m). The analysis of the elongation results is shown in Figure 49, Figure 50, Figure 51, and Figure 52 respectively. As shown in Figures 40 to 43 below, the analysis shows that the largest integral axial casings elongation is in the air compared to the seawater section which is 37.89 mm. On the other hand, as shown in the mentioned Figures, the longest integral axial casing elongation occurred in strata section 1 casing (51.2~96.2 m) is 3.555 mm.

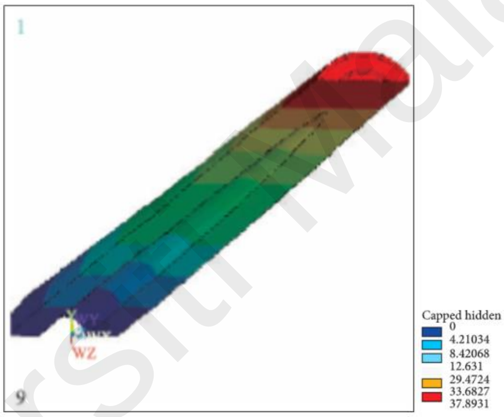

Figure 49: Casing elongation simulation result (0~51.2m).

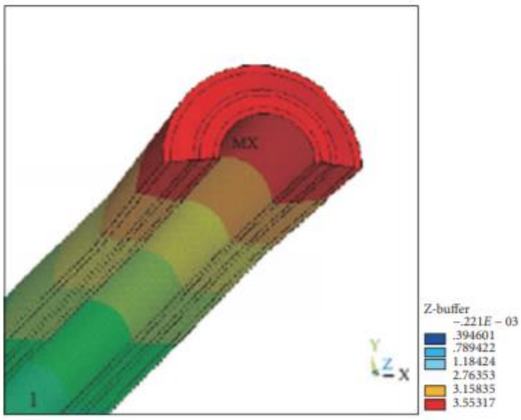

Figure 50: Casing elongation simulation result (51.2~96.2m)

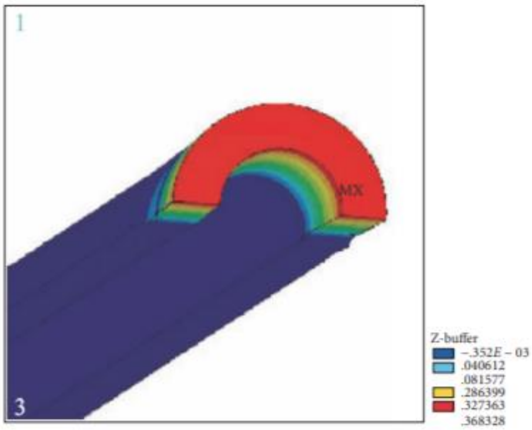

Figure 51: Casing elongation simulation result (96.2~360 m)

Figure 52: Casing elongation simulation result (360~1710 m)

Furthermore, the analysis shows, for the casing elongation in section 2 is 0.368 mm. Which is comparatively smaller to casing strata section 1. Whereas, in the elongation simulation for section 3 (360~1710 m) is 0.003m in which it is the smallest axial elongation of all, which is also can be considered negligible. However, considering the thermal expansions of the casings in different environmental conditions, which can be considered at the end, hence this section is considered to be anchored. The total elongation of the string observed is 4.281 cm. To summarise the results, the elongation of section which is air and water is more than 90% of the total elongation which is incurred. Which shows that the casing string has a binding force acting on the casing, thereby limiting and affecting the elongation.

4.6 Sea Water Temperature

Sea water temperature ranges from -1°C to 30°C with different depths of water at different temperatures at any given point or time. However, in this study the effect of sea water temperature has been neglected. This is due to, the creep deformation on oil well casing works at elevated temperatures and constant mechanical load. The average temperature of sea water however is very small compared to what is shown in Table 8 which ranges up to 270°C. Therefore, the temperature of the sea water is small enough to be negligible.

CHAPTER 5: CONCLUSION AND RECOMMENDATION

5.1 Introduction

As the demand on materials with respect to creep has increased within different applications, theories and methodologies have been developed (Kachanov, 1958). The individual event that probably has had the largest impact on the research and development within the area of creep is the establishment of nuclear power plants such as Liquid Metal Fast Breeder Reactors, LMFBR, Helium Cooled High Temperature Reactors, HTR, and Advanced Gas Cooled Reactors, AGR (Folke & Odqvist, 1974). Here, the driving force has been the very high safety requirements. In the context of high temperature pressure equipment, the weakening effect of the weldments has been recognized for several decades. In-service inspections have shown that weldments are prone to creep and fatigue damage. It is not uncommon that severely damaged weldments are revealed even before the design life of the component has been reached. In order to improve this situation actions have been taken, both from industry, universities and research institutes, aiming at an enhanced understanding of the weldment response.

However, wellhead uplift was detected during the pilot test among many thermal injection wells. Based on field measuring, the average wellhead uplift is 4~5 cm with the highest reaching 24.5 cm. As the last firewall for oil well safety, Christmas tree should be paid special attention and protected with all kinds of safety precautions the main requirements to casing that provides cementing of oil and gas wells during drilling and operation is their optimum centralisation, which allows achieving a better homogeneity of the slurry flow in the annulus. Optimum standoff between the borehole wall and the casing is ensured with special devices, centralizers put on the casing and spaced along it in a certain pattern. The paper offers a numerical solution to the centralisation of casing.

The model includes 3D dynamic equations of the lateral and axial motion of a long pipe in the wellbore with constrained deflections in borehole during tripping operation considering all the major factors typical for casing exploration. A numerical method that enables to determine contact and friction forces as well as standoff between the borehole wall and the casing is proposed (Folke & Odqvist, 1974). Isotropic creep damage models and their applications for crack growth analysis have been shown in this section. These creep damage models generally consist of creep constitutive equation and creep damage evolution equations. According to the difference of damage evolution equations, the creep damage models can be divided into two groups: one is the stress-based creep damage model and the other is the strain-based creep damage model (Norton, 1929).

The ideal centralization of casing that provides cementing of oil and gas wells during drilling and operation is one of the most important criteria, as it allows for greater slurry flow homogeneity in the annulus. Special devices, called centralisers, are placed on the casing and spaced in a certain pattern to guarantee optimal standoff between the borehole wall and the casing. The centralisation of casing is solved numerically in this study. The ideal centralization of casing that provides cementing of oil and gas wells during drilling and operation is one of the most important criteria, as it allows for greater slurry flow homogeneity in the annulus. Special devices, called centralizers, are placed on the casing and spaced in a certain pattern to guarantee optimal standoff between the borehole wall and the casing.

5.2 Conclusion

To conclude, this research focussed on what was found in this study is that how the creep deformation actually exists and propagates through the history of the oil well casing. Subsequently, in such cases such as when the creep deformation exists, how does it occur and what causes it. For oil well casing, it is subject to extreme pressure and temperature especially during the fracturing processes and well steam injection processes. Such environmental variables affect the microstructure of the oil well casing and thus advancing to become creep deformation over time. Current studies do not suggest or proves any additional effect of these stresses on the oil well casing materials, even, within the limits of yield strength of the material yet over some period of time and causes irreversible plastic deformation

Firstly, as shown in the simulation results above, the maximum total deformation that was experienced by the casing was $1.4645 \times 10^{-7} m$ which indicates that the elongation experienced by the casing is very small. Average elastic strain was 1.084×10^{-8} *m/m*, whereas the average volumetric change is $0.30042\ m^3$.

Secondly, by simulating the 3D finite element model, each section was analysed on their casing stresses and elongations respectively. Each section represented the different environmental conditions which was taken account in the simulation conditions to achieve greater results.

Thirdly, A majority of the total elongation occurs in one of the sections which is seawater. Analysis shows that around 88% of the elongation belongs to the section. The other parts of the casing strings such as below 360 m were the least comparatively. Therefore, least amount of elongation was found in that anchored section.

The main requirements to casing that provides cementing of oil and gas wells during drilling and operation is their optimum centralisation, which allows achieving a better homogeneity of the slurry flow in the annulus. Optimum standoff between the borehole wall and the casing is ensured with special devices, centralizers put on the casing and spaced along it in a certain pattern. This paper offered a numerical solution to the centralisation of casing. The model includes 3D dynamic equations of the lateral and axial motion of a long pipe in the wellbore with constrained deflections in borehole during tripping operation considering all the major factors typical for casing exploration. It was indicated that the failure time predicted by Dyson damage model was found to be half the power law models at the lowest stress level and the Dyson damage model was a method to consistently give conservative failure life. As what we have discussed in chapter one of this paper, the assumption of a constant stress exponent in power law models was erroneous due to the possible change in the deformation mechanism. Furthermore, the Dyson model was shown not to be subject to this behaviour due to the use of a sinh function. (T. H. Hyde et al., 2006; Kachanov, 1958) made a comparison between Kachanov-Rabotnov damage model and Kowalewski-Hayhurst-Dyson damage model to the stress analysis of thin-walled structures.

Multiple components such as pipes, used in multiple industries (i.e., chemical plants, power plants etc.) which are mainly exposed to higher temperatures. Therefore, determining the life of these components during the designing stage is crucial. Significant advancements in creep modelling for life prediction and crack growth analysis have been made in the past few decades. These details provide a wide window of realistic details at the damage mechanics in the creep processes. These details serve a great purpose of providing users into the key ideas, features and other important details of the damage mechanism. As known generally, creep failure is mostly occurred in high temperature components or environmental conditions. Cracks have often been detected and propagated in most welded structures operating at high temperatures. In general, hydraulic fracturing is the biggest factor in terms of causing deformation to the casings. Fracturing processes causes structural stresses that lead to wellbore integrity decline (Davies et al., 2014; Mohammed et al., 2019). Both Q. Wang et al. (2018) and Xi et al. (2018) mentions that additional load and stresses are experienced by the casing during the fracturing processes which results in casing damage under the action of formation shear slip. Both pointed out that fracture slip during hydraulic fracturing can cause shear slip

5.3 Contribution to Knowledge

With the successful implementation of this research project, this report will contribute to the application of Structural Analysis simulations in the studies of Oil well Creep Deformation dynamics as a case study for future research reference and expand the study to more in-depth. The primary aim of the researcher in this study is to relook at the creep deformation of oil well casing from a new perspective. So far, most studies on creep deformation have been studied in mostly Gas plants and microstructure of electrical components. However, in this paper, researcher have shifted the focus to creep mechanism at work in oil well casings.

5.4 Future Works

Future works beyond this research project should further demonstrate the extensibility of the simulation by implementing additional variants of Creep Deformation dynamics systems (e.g., Seawater temperature, vibrations, thermal expansion, and etc.) and also to simulate the model in 3-D of the effect, where it will simulate the unforeseen creep deformation pattern and failure mechanism at work. Suggestion for continuing this research, which will be extended with multiple variables such as seawater temperature and multiple type of materials including J55. The comparison of the samples will be compared in different environments and different stages of their life in order to analyse the creep deformation mechanism in act. Such results will be tabulated and compared with the Computational Aided Analysis as well as its method to mitigate such deformations.

REFERENCES

Aasen, J. A., & Pollard, M. (2003). Casing Design–Review of Design Methodology.

Bastola, A., Wang, J., Mirzaee-Sisan, A., & Njuguna, J. (2014). *Predicting hydrostatic collapse of pipes using finite element analysis.* Paper presented at the ASME 2014 33rd International Conference on Ocean, Offshore and Arctic Engineering.

Bolton, J. (2008). Analysis of structures based on a characteristic-strain model of creep. *International journal of pressure vessels and piping, 85*(1), 108-116. doi:https://doi.org/10.1016/j.ijpvp.2007.06.013

Bolton, J. (2011). The extrapolation of creep rupture data by PD6605 – An independent case study. *International journal of pressure vessels and piping, 88*(4), 158-165. doi:https://doi.org/10.1016/j.ijpvp.2011.03.001

Browne, R., Cane, B., Parker, J., & Walters, D. (1981). Creep failure analysis of butt welded tubes. In *Creep and fracture of engineering materials and structures*.

Chen, Z., Shi, L., & Xiang, D. (2017). Mechanism of casing deformation in the Changning–Weiyuan national shale gas demonstration area and countermeasures. *Natural Gas Industry B, 4*(1), 1-6.

Chen, Z., Zhu, W., & Di, Q. (2018). Elasticity solution for the casing under linear crustal stress. *Engineering failure analysis, 84*, 185-195.

Cirimello, P. G., Otegui, J. L., Carfi, G., & Morris, W. (2017). Failure and integrity analysis of casings used for oil well drilling. *Engineering failure analysis, 75*, 1-14.

Coleman, M. C., Parker, J. D., & Walters, D. J. (1985). The behaviour of ferritic weldments in thick section 12Cr12Mo14V pipe at elevated temperature. *International journal of pressure vessels and piping, 18*(4), 277-310. doi:https://doi.org/10.1016/0308-0161(85)90015-8

CROOK, R., KULAKOFSKY, D., & GRIFFITL, J. (2003). Tailor lightweight slurry designs to well conditions and production plans: Drilling report. *World oil, 224*(10), 44-51.

Dall'Acqua, D., Hodder, M., & Kaiser, T. (2013). Burst and collapse responses of production casing in thermal applications. *SPE Drilling & Completion, 28*(01), 93-104.

Davies, R. J., Almond, S., Ward, R. S., Jackson, R. B., Adams, C., Worrall, F., . . . Whitehead, M. A. (2014). Oil and gas wells and their integrity: Implications for shale and unconventional resource exploitation. *Marine and Petroleum Geology, 56*, 239-254. doi:https://doi.org/10.1016/j.marpetgeo.2014.03.001

Dusseault, M. B., Bruno, M. S., & Barrera, J. (2001). Casing shear: causes, cases, cures. *SPE Drilling & Completion, 16*(02), 98-107.

Dusseault, M. B., Maury, V., Sanfilippo, F., & Santarelli, F. J. (2004). *Drilling around salt: risks, stresses, and uncertainties.* Paper presented at the Gulf Rocks 2004, the 6th North America Rock Mechanics Symposium (NARMS).

Fan, B., Deng, J., Tan, Q., & Liu, W. (2018). *Laboratory study on hydraulic fracturing in poorly consolidated sandstones.* Paper presented at the 52nd US Rock Mechanics/Geomechanics Symposium.

Fang, J., Wang, Y., & Gao, D. (2015). On the collapse resistance of multilayer cemented casing in directional well under anisotropic formation. *Journal of Natural Gas Science and Engineering, 26*, 409-418.

Farmer, P., Miller, D., Pieprzak, A., Rutledge, J., & Woods, R. (1996). Exploring the subsalt. *Oilfield Review, 8*.

Ferla, A., Lavrov, A., & Fjær, E. (2009). *Finite-element analysis of thermal-induced stresses around a cased injection well.* Paper presented at the Journal of Physics: Conference Series.

Fleckenstein, W., Eustes, A., & Miller, M. (2001). Burst-induced stresses in cemented wellbores. *SPE Drilling & Completion, 16*(02), 74-82.

Folke, K., & Odqvist, G. (1974). Mathematical theory of creep and creep rupture. *Claredon Oxford*.

Furui, K., Fuh, G.-F., Abdelmalek, N. A., & Morita, N. (2010). A comprehensive modeling analysis of borehole stability and production-liner deformation for inclined/horizontal wells completed in a highly compacting chalk formation. *SPE Drilling & Completion, 25*(04), 530-543.

Guan, K., Xu, H., & Wang, Z. (2005). Quantitative study of creep cavity area of HP40 furnace tubes. *Nuclear Engineering and Design, 235*(14), 1447-1456. doi:https://doi.org/10.1016/j.nucengdes.2005.01.009

Guo, K., Li, H., & Yu, Z. (2016). In-situ heavy and extra-heavy oil recovery: A review. *Fuel, 185*, 886-902.

Guo, Y., Blanford, M., & Candella, J. (2015). Evaluating the risk of casing failure caused by high-density perforation: a 3D finite-element-method study of compaction-induced casing deformation in a deepwater reservoir, Gulf of Mexico. *SPE Drilling & Completion, 30*(02), 141-151.

Hamilton, K., & Pattillo, P. D. (2019). *Developing an evaluation method for casing connections used in hydraulically fractured wells.* Paper presented at the SPE Hydraulic Fracturing Technology Conference and Exhibition.

Hayhurst, D. (1972). Creep rupture under multi-axial states of stress. *Journal of the Mechanics and Physics of Solids, 20*(6), 381-382.

Hayhurst, D., & Webster, G. (1986a). An overview of studies of stress state effects during creep of circumferentially notched bars, Techniques for Multiaxial Creep Testing, edited by DJ Gooch and IM How. *Ed. Gooch, DJ, and How, IM, Elsevier Applied Science, Amsterdam*, 137-175.

Hayhurst, D., & Webster, G. (1986b). An overview on studies of stress state effects during creep of circumferentially notched bars. *Techniques for multiaxial creep testing*, 137-175.

Hayhurst, D. R., Vakili-Tahami, F., & Zhou, J. Q. (2003). Constitutive equations for time independent plasticity and creep of 316 stainless steel at 550°C. *International journal of pressure vessels and piping, 80*(2), 97-109. doi:https://doi.org/10.1016/S0308-0161(03)00027-9

Hayhurst, R., Mustata, R., & Hayhurst, D. (2005). Creep constitutive equations for parent, Type IV, R-HAZ, CG-HAZ and weld material in the range 565–640 C for Cr–Mo–V weldments. *International journal of pressure vessels and piping, 82*(2), 137-144.

Hore, S., & Ghosh, R. (2011). Computer simulation of the high temperature creep behaviour of Cr–Mo steels. *Materials Science and Engineering: A, 528*(19-20), 6095-6102.

Hyde, C. J., Hyde, T. H., Sun, W., & Becker, A. A. (2010). Damage mechanics based predictions of creep crack growth in 316 stainless steel. *Engineering Fracture Mechanics, 77*(12), 2385-2402. doi:https://doi.org/10.1016/j.engfracmech.2010.06.011

Hyde, T. H., Becker, A. A., Sun, W., & Williams, J. A. (2006). Finite-element creep damage analyses of P91 pipes. *International journal of pressure vessels and piping, 83*(11), 853-863. doi:https://doi.org/10.1016/j.ijpvp.2006.08.013

Ichim, A., Marquez, A., & Teodoriu, C. (2016). *How accurate is your well integrity? A discussion about the surface casing integrity under temperature loading in heavy oil fields.* Paper presented at the SPE Latin America and Caribbean Heavy and Extra Heavy Oil Conference.

Ichim, A., & Teodoriu, C. (2016). *Revisiting thermal well integrity through a closer look at casing-cement-formation interaction.* Paper presented at the SPE Thermal Well Integrity and Design Symposium.

Ivarsson, B., & Sandström, R. (1980). Creep deformation and rupture of butt-welded tubes of cold-worked AISI 316 steel. *Metals Technology, 7*(1), 440-448.

Kachanov, L. (1958). On the rupture time under the condition of creep. *Izv. Akad. Nauk SSSR, Otd. Tekh. Nauk, 8*, 26.

Kalil, I. A., & McSpadden, A. R. (2012). Casing burst stresses in particulate-filled annuli: where is the cement? *SPE Drilling & Completion, 27*(04), 473-485.

Kiran, R., Teodoriu, C., Dadmohammadi, Y., Nygaard, R., Wood, D., Mokhtari, M., & Salehi, S. (2017). Identification and evaluation of well integrity and causes of failure of well integrity barriers (A review). *Journal of Natural Gas Science and Engineering, 45*, 511-526.

Kuanhai, D., Wanying, L., Tianguo, X., Dezhi, Z., Ming, L., & Yuanhua, L. (2017). Experimental study the collapse failure mechanism of cemented casing under non-uniform load. *Engineering failure analysis, 73*, 1-10.

Leinster, M. G. (2008). A method of creep rupture data extrapolation based on physical processes. *International journal of pressure vessels and piping, 85*(10), 701-710. doi:https://doi.org/10.1016/j.ijpvp.2008.03.001

Lim, T. K., Tellier, E., & Howells, H. (2012). Wellhead, Conductor and Casing Fatigue–Causes and Mitigation. *Proc. Deep Offshore Technology (DOT).*

Lin, T., Zhang, Q., Lian, Z., Chang, X., Zhu, K., & Liu, Y. (2016). Evaluation of casing integrity defects considering wear and corrosion–Application to casing design. *Journal of Natural Gas Science and Engineering, 29*, 440-452.

Liu, S., Zheng, H., Zhu, X., & Tong, H. (2014). Equations to calculate collapse strength of defective casing for steam injection wells. *Engineering failure analysis, 42*, 240-251.

Liu, W., Yu, B., & Deng, J. (2017). Analytical method for evaluating stress field in casing-cement-formation system of oil/gas wells. *Applied Mathematics and Mechanics, 38*(9), 1273-1294.

Liu, Z., Samuel, R., Gonzales, A., & Kang, Y. (2018). *Analysis of casing fatigue failure during multistage fracturing operations.* Paper presented at the Abu Dhabi International Petroleum Exhibition & Conference.

Ma, Y., Shim, S., & Yoon, K. (2009). Assessment of power law creep constants of Gr91 steel using small punch creep tests. *Fatigue & Fracture of Engineering Materials & Structures, 32*(12), 951-960.

Mao, L., Cai, M., & Wang, G. (2018). Effect of rotation speed on the abrasive–erosive–corrosive wear of steel pipes against steel casings used in drilling for petroleum. *Wear, 410*, 1-10.

Marriott, D. (1992). Current trends in high temperature design. *International journal of pressure vessels and piping, 50*(1-3), 13-35.

Mohammed, A. I., Oyeneyin, B., Atchison, B., & Njuguna, J. (2019). Casing structural integrity and failure modes in a range of well types - A review. *Journal of Natural Gas Science and Engineering, 68*, 102898. doi:https://doi.org/10.1016/j.jngse.2019.05.011

Nickel, H., Schubert, F., Penkalla, H., & Breitbach, G. (1991). Aspects of design codes for metallic high temperature components. *International journal of pressure vessels and piping, 47*(2), 167-192.

Norton, F. H. (1929). *The creep of steel at high temperatures*: McGraw-Hill Book Company, Incorporated.

Noshi, C., Noynaert, S., & Schubert, J. (2018). *Casing failure data analytics: A novel data mining approach in predicting casing failures for improved drilling* *performance and production optimization.* Paper presented at the SPE Annual Technical Conference and Exhibition.

Olarte Caro, D. P., Marquez, L. J., Landinez, G. A., & Amaya, R. (2009). *Casing collapse study on block VI wells: Casabe field.* Paper presented at the Latin American and Caribbean Petroleum Engineering Conference.

Pearce, J., Legrand, P., Dominique, T., Childers, B., Rambow, F., & Dria, D. (2009). *Real-time compaction monitoring with fiber-optic distributed strain sensing (DSS).* Paper presented at the SPWLA 50th Annual Logging Symposium.

Plaxton, B., Pehlke, T., Baxter, D., Crockett, M., & Kaiser, T. (2018). *SAGD production casing failure diagnosis and repair.* Paper presented at the SPE Thermal Well Integrity and Design Symposium.

Sathuvalli, U. B., & Suryanarayana, P. (2016). Structural-casing/soil interaction effects on wellhead motion. *SPE Drilling & Completion, 31*(04), 273-285.

Sedmak, A., Arsić, M., Šarkoćević, Ž., Medjo, B., Rakin, M., Arsić, D., & Lazić, V. (2020). Remaining strength of API J55 steel casing pipes damaged by corrosion. *International journal of pressure vessels and piping, 188*, 104230. doi:https://doi.org/10.1016/j.ijpvp.2020.104230

Smith, D. J., Walker, N. S., & Kimmins, S. T. (2003). Type IV creep cavity accumulation and failure in steel welds. *International journal of pressure vessels and piping, 80*(9), 617-627. doi:https://doi.org/10.1016/S0308-0161(03)00134-0

Spindler, M. W. (2005). The prediction of creep damage in type 347 weld metal. Part I: the determination of material properties from creep and tensile tests. *International journal of pressure vessels and piping, 82*(3), 175-184. doi:https://doi.org/10.1016/j.ijpvp.2004.09.003

Teodoriu, C., Ulmanu, V., & Badicioiu, M. (2008). *Casing fatigue life prediction using local stress concept: theoretical and experimental results.* Paper presented at the SPE Western Regional and Pacific Section AAPG Joint Meeting.

Torbergsen, H.-E. B., Haga, H. B., Sangesland, S., Aadnøy, B. S., Sæby, J., Johnsen, S., . . . Lundeteigen, M. A. (2012). An introduction to well integrity. *Trondheim: NTNU https://www. norskoljeoggass. no/Global/2013% 20Dokumenter/Andre% 20vedlegg/INTRODUCTION% 20TO% 20WELL% 20INTEGRITY.*

Viswanathan, R. (1989). *Damage mechanisms and life assessment of high temperature components*: ASM international.

Vudovich, A., Chin, L., & Morgan, D. (1988). *Casing deformation in Ekofisk.* Paper presented at the Offshore Technology Conference.

Wang, H., & Samuel, R. (2016). 3D geomechanical modeling of salt-creep behavior on wellbore casing for presalt reservoirs. *SPE Drilling & Completion, 31*(04), 261-272.

Wang, Q., Zhang, L., & Hu, J. (2018). Real-time risk assessment of casing-failure incidents in a whole fracturing process. *Process Safety and Environmental Protection, 120*, 206-214.

Weber, H., & Bendick, W. (1992). *Entwicklung einer Zeitstandschädigung und ihre Auswirkung auf das Bauteilverhalten.* Paper presented at the VGB Conf. Residual Service Life 1992.

Webster, G. A., & Ainsworth, R. A. (2013). *High temperature component life assessment*: Springer Science & Business Media.

Williams, J., Coleman, M., & Walters, D. (1984). *Weld performance factors for high temperature welded components.* Paper presented at the Proceedings of the second international conference on creep and fracture of engineering materials and structures held at University College, Swansea, 1st-6th April, 1984.

Wilshire, B., & Burt, H. (2008). Damage evolution during creep of steels. *International journal of pressure vessels and piping, 85*(1), 47-54. doi:https://doi.org/10.1016/j.ijpvp.2007.06.002

Wilshire, B., & Scharning, P. J. (2008). Extrapolation of creep life data for 1Cr–0.5Mo steel. *International journal of pressure vessels and piping, 85*(10), 739-743. doi:https://doi.org/10.1016/j.ijpvp.2008.04.002

Wu, J., & Knauss, M. E. (2006). *Casing temperature and stress analysis in steam-injection wells.* Paper presented at the International Oil & Gas Conference and Exhibition in China.

Wu, Y., Guo, B., & Zhang, J. (2017). Analysis and simulation of metal casing effect on induction logging. *Optik, 138*, 302-313.

Xi, Y., Li, J., Liu, G., Cha, C., & Fu, Y. (2018). Numerical investigation for different casing deformation reasons in Weiyuan-Changning shale gas field during multistage hydraulic fracturing. *Journal of Petroleum Science and Engineering, 163*, 691-702.

Xiangxin, L., Xueren, Z., & Xiaojun, Y. (2003). The finite element analysis of HLCF life prediction for PM FGH95 based on damage mechanics. *Journal of Aero- space Power, 18*(1), 101-108.

Xie, J., & Liu, Y. (2008). *Analysis of Casing Deformations in Thermal Wells.* Paper presented at the Abaqus Users' Conference, RI.

Xu, Y., Yang, Q., Li, Q., & Chen, B. (2006). *The Oil Well Casing's Anti-Corrosion and Control Technology of Changqing Oilfield.* Paper presented at the International Oil & Gas Conference and Exhibition in China.

Yan, W., Zou, L., Li, H., Deng, J., Ge, H., & Wang, H. (2017). Investigation of casing deformation during hydraulic fracturing in high geo-stress shale gas play. *Journal of Petroleum Science and Engineering, 150*, 22-29.

Yin, F., Deng, Y., He, Y., Gao, D., & Hou, B. (2018). Mechanical behavior of casing crossing slip formation in waterflooding oilfields. *Journal of Petroleum Science and Engineering, 167*, 796-802.

Yin, F., & Gao, D. (2015). Prediction of sustained production casing pressure and casing design for shale gas horizontal wells. *Journal of Natural Gas Science and Engineering, 25*, 159-165.

Yin, F., Han, L., Yang, S., Deng, Y., He, Y., & Wu, X. (2018). Casing deformation from fracture slip in hydraulic fracturing. *Journal of Petroleum Science and Engineering, 166*, 235-241.

Yin, F., Xiao, Y., Han, L., & Wu, X. (2018). Quantifying the induced fracture slip and casing deformation in hydraulically fracturing shale gas wells. *Journal of Natural Gas Science and Engineering, 60*, 103-111.

Yuan, Z., Schubert, J., Teodoriu, C., & Gardoni, P. (2012). *HPHT gas well cementing complications and its effect on casing collapse resistance.* Paper presented at the SPE Oil and Gas India Conference and Exhibition.

Zhang, G., Zhao, Y., Xue, F., Mei, J., Wang, Z., Zhou, C., & Zhang, L. (2011). Creep–fatigue interaction damage model and its application in modified 9Cr–1Mo steel. *Nuclear Engineering and Design, 241*(12), 4856-4861. doi:https://doi.org/10.1016/j.nucengdes.2011.08.076

Zhang, Q., Lian, Z., Lin, T., Deng, Z., Xu, D., & Gan, Q. (2016). Casing wear analysis helps verify the feasibility of gas drilling in directional wells. *Journal of Natural Gas Science and Engineering, 35*, 291-298.

Zhao, H., Chen, M., & Wang, J. (2011). Salt loading on casing in cased wellbore sections. *International journal of rock mechanics and mining sciences (1997), 48*(3), 501-505.